

# Drive-by-wireless for Vehicle Control and Monitor using Wireless Controller Area Network (WCAN)

S.Srinath

B. Tech Student, School of Electronics Engineering  
Vellore Institute of Technology  
Vellore, India  
srinath.s2011@vit.ac.in

Gerardine Immaculate Mary

Assistant Professor (Selection Grade)  
Vellore Institute of Technology  
Vellore, India  
gerardine@vit.ac.in

**Abstract**—Wired systems are complex, heavy, less secure and expensive. Hence, in today's 21<sup>st</sup> century wireless technology has been gradually adopted by automobile manufacturers. A vehicle has various control units which were connected using traditional point-to-point wiring architecture in olden days. These were replaced by a CAN bus later. This paper uses Wireless CAN (WCAN) to interconnect various control units. This has several important advantages such as system flexibility, message routing, filtering, multicast, together with data consistency. This paper proposes a drive-by-wireless technique for vehicle control and monitor functions using Wireless Controller Area Network. Traditional hydraulic or mechanical methods of steering, braking and accelerating of a vehicle will be replaced by Drive by Wireless Technique. Also, traditional vehicle monitoring methods are done in a wireless manner. The algorithm includes Unique Identification Codes which is sent with all the transactions involving wireless communication packets to reduce interference from adjacent drive-by-wireless system.

**Keywords**- Drive-by-wireless; WCAN; Vehicle Control and Monitor; Unique Identification Codes

## I. INTRODUCTION

Drive-by-wireless techniques replace the mechanical and hydraulic connections between the driver and the associated vehicle actuators with electronic communication systems. These systems transmit electronic messages to direct a vehicle component based on the action taken by the driver of the vehicle, e.g., turning a steering wheel, pressing a brake pedal, or pressing an accelerator pedal [1]. In the past the vehicle bus communication used point to point communication wiring systems which causes complexity, bulkiness, is expensive with increasing electronics and controller deployed vehicles. The abundance of wiring required makes the whole circuit complicated. CAN solves this complexity by using twisted pair cables that is shared throughout the control. Not only does it reduce the wiring complexity but it also made it possible to interconnect several devices using only single pair of wires and allowing them to have simultaneous data exchange. WCAN has several important advantages such as system flexibility, message routing, filtering, multicast, together with data consistency [2]. The new WCAN is proposed to

exploit the advantages of CAN and still providing wireless access. The rest of the paper is organized as follows; section II outlines the related work and Drive-by-wireless technique, section III describes the block diagram of the system, section IV briefs on the components used, section V presents the circuit diagram of the system, section VI discusses algorithm, section VII presents the hardware output and section VIII briefs the conclusion.

## II. RELATED WORK AND DRIVE-BY-WIRELESS TECHNIQUE

Stähle et. Al [1] investigated the so-called drive-by-wireless, i.e., using a wireless network to control steering, braking, accelerating and other functions within an automobile. Mary et.al [2] showed that WCAN is suited for real time control applications giving maximum throughput for minimal latency for an optimized number of nodes. Iturri et. Al [11] showed that ZigBee is a viable technology for successfully deploying intra-car wireless sensor networks. Lin et. Al [3] proposed an Intra-car Wireless Sensor Network (WSN) to eliminate the amount of wiring harness and simplify the wiring structure. Lin et. Al [6] evaluated the performance of intra-vehicular wireless sensor networks (IVWSNs) under interference from WiFi and Bluetooth devices. Torbitt et. Al [7] analyzed the surface wave hypothesis at different frequencies in intra-vehicular environments. Ahmed et. Al [8] investigated the issues around replacing the current wired data links between electrical control units (ECU) and sensors/switches in a vehicle, with wireless links. Lin et. Al [9] proposed a new wireless technology known as Bluetooth Low Energy (BLE) and outlined a new architecture for IVWSN. This paper proposes Drive-by-wireless technique using WCAN.

### A. Drive-by-wire System

Drive-by-wire technology in the automotive industry is the use of electrical or electro-mechanical systems for performing vehicle functions traditionally achieved by mechanical linkages. This technology replaces the traditional mechanical control systems with electronic control systems using electromechanical actuators and human-machine interfaces such as pedal and steering feel emulators. The Drive-by-wire system used point to point

communication wiring systems as shown in Figure 1. This causes complexity, heaviness and is expensive.

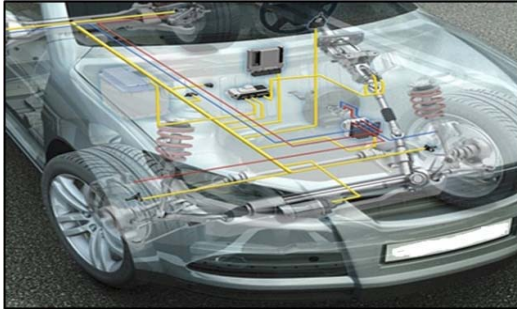


Figure 1. Existing System

### B. Drive-by-wireless System

The Drive-by-wireless system ensures less weight, safety and comfort. The position of the sensor, motor and the wheel for the proposed Drive-by-wireless system is shown in Figure 2.

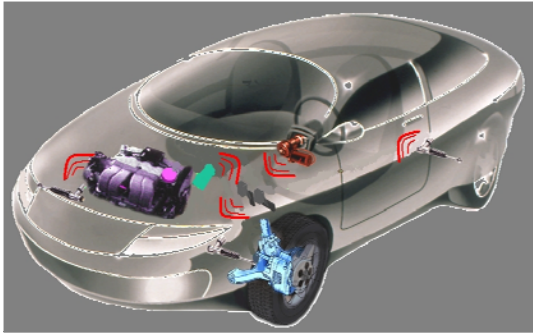


Figure 2. Drive-by-wireless System

### III. BLOCK DIAGRAM OF THE PROPOSED SYSTEM

The block diagram of the system is presented in Figure 3. The system has four microcontroller units and ZigBee over 802.15.4 protocol is used for wireless communication.

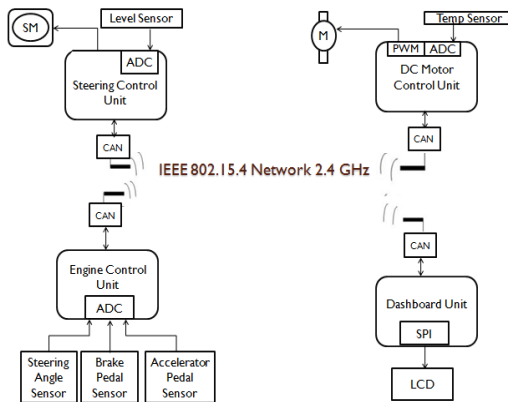


Figure 3. Block Diagram

The Steering, Brake, Accelerator sensors are associated with the Engine Control Unit. The Dashboard

unit contains the LCD, the D.C. Motor unit contains a D.C. motor with a motor drive and a temperature sensor. Finally, the Servo Motor Unit contains a Servo Motor and a level sensor.

### IV. COMPONENTS DESCRIPTION

PIC18F45K22 is the microcontroller used in the project. Circular potentiometers are used for Brake-Acceleration and Steering. Servo Motor and a level sensor is used for the Servo Motor Unit and DC Motor unit contains a D.C. motor with a motor drive and a temperature sensor. LCD Display is used for displaying the engine temperature and fuel levels.

#### A. PIC18F45K22

PIC18(L)F45K22 has 32k program memory, 1536 bytes of SRAM and 256bytes of EEPROM. It has three 8-bit timers and four 16-bit timers. All of the devices in the PIC18(L)F2X/4XK22 family offer ten different oscillator options, allowing users a wide range of choices in developing application hardware. These include:

- Four Crystal modes, using crystals or ceramic resonators
- Two External Clock modes, offering the option of using two pins (oscillator input and a divide-by-4 clock output) or one pin (oscillator input, with the second pin reassigned as general I/O)
- Two External RC Oscillator modes with the same pin options as the External Clock modes
- An internal oscillator block which contains a 16 MHz HFINTOSC oscillator and a 31 kHz LFINTOSC oscillator, which together provide eight user selectable clock frequencies, from 31 kHz to 16 MHz. This option frees the two oscillator pins for use as additional general purpose I/O.
- A Phase Lock Loop (PLL) frequency multiplier, available to both external and internal oscillator modes, which allows clock speeds of up to 64 MHz. Used with the internal oscillator, the PLL gives users a complete selection of clock speeds, from 31 kHz to 64 MHz – all without using an external crystal or clock circuit.

40-pin PDIP

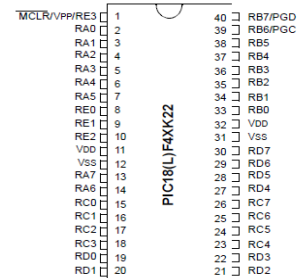


Figure 4. PIC18F45K22 Microcontroller

#### B. Potentiometers

A potentiometer is a three terminal resistor with a sliding contact forms an adjustable voltage divider and only two terminals are used one end and the wiper acts as a variable resistor or rheostat. Electric potential is measured by potentiometer device.

### C. LCD Display

The HD44780U dot-matrix liquid crystal display controller and driver LSI displays alphanumeric, Japanese kana characters, and symbols. It can be configured to drive a dot-matrix liquid crystal display under the control of a 4- or 8-bit microprocessor. Since all the functions such as display RAM, character generator, and liquid crystal driver, required for driving a dot-matrix liquid crystal display are internally provided on one chip, a minimal system can be interfaced with this controller/driver. A single HD44780U can display up to one 8-character line or two 8-character lines. The HD44780U has pin function compatibility with the HD44780S which allows the user to easily replace an LCD-II with an HD44780U. The HD44780U character generator ROM is extended to generate 208 5x8 dot character fonts and 32 5 x10 dot character fonts for a total of 240 different character fonts. The low power supply (2.7V to 5.5V) of the HD44780U is suitable for any portable battery-driven product requiring low power dissipation.

### D. DC Motor

A DC motor has a two wire connection. All drive power is supplied over these wires. Most DC motors are pretty fast of about 5000 rpm. The DC motor speed is controlled by a technique called pulse width modulation or PWM.



Figure 5. D.C. Motor

### E. Servo Motor

The function of the servo is to receive a control signal that represents a desired output position of the servo shaft, and apply power to its DC motor until the shaft turns to that position. It uses position sensing device to rotate the shaft. The shaft can turn a maximum of 200 degree so back and forth.



Figure 6. Servo Motor

### F. Pressure Sensor

The MPX5010/MPXV5010G series piezoresistive transducers are state-of-the-art monolithic silicon pressure sensors designed for a wide range of applications, but

particularly those employing a microcontroller or microprocessor with A/D inputs. This transducer combines advanced micromachining techniques, thin-film metallization, and bipolar processing to provide an accurate, high level analog output signal that is proportional to the applied pressure.

Its features are

- . 5.0% Maximum Error over 0° to 85°C
- . Ideally Suited for Microprocessor or Microcontroller-Based Systems
- . Durable Epoxy Unibody and Thermoplastic (PPS) Surface Mount Package
- . Temperature Compensated over .40° to +125°C

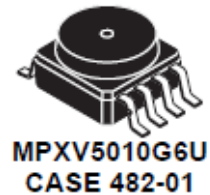


Figure 7. Pressure Sensor

### G. Temperature Sensor

The LM35 series are precision integrated-circuit temperature sensors, whose output voltage is linearly proportional to the Celsius (Centigrade) temperature. The LM35 thus has an advantage over linear temperature sensors calibrated in ° Kelvin, as the user is not required to subtract a large constant voltage from its output to obtain convenient Centigrade scaling. The LM35 does not require any external calibration or trimming to provide typical accuracies of  $\pm 1/4^\circ\text{C}$  at room temperature and  $\pm 3/4^\circ\text{C}$  over a full  $-55$  to  $+150^\circ\text{C}$  temperature range. Low cost is assured by trimming and calibration at the wafer level. The LM35's low output impedance, linear output, and precise inherent calibration make interfacing to readout or control circuitry especially easy. It can be used with single power supplies, or with plus and minus supplies. As it draws only 60  $\mu\text{A}$  from its supply, it has very low self-heating, less than  $0.1^\circ\text{C}$  in still air. The LM35 is rated to operate over a  $-55^\circ$  to  $+150^\circ\text{C}$  temperature range, while the LM35C is rated for a  $-40^\circ$  to  $+110^\circ\text{C}$  range ( $-10^\circ$  with improved accuracy). The LM35 series is available packaged in hermetic TO-46 transistor packages, while the LM35C, LM35CA, and LM35D are also available in the plastic TO-92 transistor package. The LM35D is also available in an 8-lead surface mount small outline package and a plastic TO-220 package.

### H. CAN MCP2515

It is a Stand-Alone CAN Controller with SPI Interface, 18 pin I.C.

- Implements CAN V2.0B at 1 Mb/s: 0 – 8 byte length in the data field, Standard and extended data and remote frames
- Receive Buffers, Masks and Filters:  
Two receive buffers with prioritized message Storage, Six 29-bit filters and Two 29-bit masks

- Data Byte Filtering on the First Two Data Bytes (applies to standard data frames)
- Three Transmit Buffers with Prioritization and Abort Features
- High-Speed SPI Interface (10 MHz): SPI modes 0,0 and 1,1
- One-Shot mode Ensures Message Transmission is Attempted Only One Time
- Clock Out Pin with Programmable Prescaler: Can be used as a clock source for other device(s)
- Start-of-Frame Signal is Available for Monitoring the SOF Signal: Can be used for time-slot-based protocols and/or bus diagnostics to detect early bus degradation

## V. CIRCUIT DIAGRAM

The system comprises of four control units which communicate with each other using Zigbee over 802.15.4 protocol. The four modules are Engine Control Unit, D.C. Motor Unit, Servo Motor Unit and the Dashboard Unit.

The input 220V A.C. power supply is converted to 12V D.C. by an adapter. Various units in the modules require only 5V D.C and 3.3 V D.C. power supply. Hence a regulator is used for this purpose. The PIC18F45K22 microcontroller is a 40 pin I.C. There are 5 ports. Port A, B, C and D have 8 pins each while Port E has 3 pins. The remaining 5 pins are used for MCLR, VDD and Ground. The ICSP (In Circuit Serial Programmer) is a 5 pin device which is used by PitKit 3 to dump the program from the computer to the microcontroller. Pin 1 of the ICSP is connected to a high voltage to erase any previous programs, Pin 2 is the clock, Pin 3 is the data, Pin 4 is connected to Ground while Pin 5 is connected to VDD.

The Dashboard Module circuit diagram is shown in Figure 8. It consists of a 16x2 LCD display.

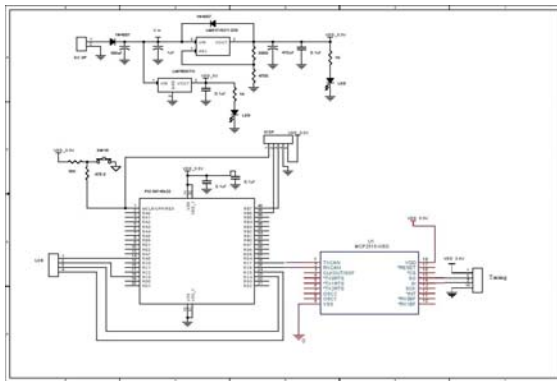


Figure 8. The Dashboard Module

SP1 and SP2 of the PIC18F45K22 are pins A5, C3, C4, C5 and A6, C3, C4, C5 respectively. A5 and A6 are the Enable Pin, C3 is the clock, C4 is the Data Input and C5 is the Data Output. UART1 and UART2 are pins 25, 26 and 29, 30 respectively. 25 and 29 are for transmission while 26 and 30 are for reception. In CAN, CANL is for transmission and CANH is for reception. In Zigbee Pin 2 is for transmission and Pin 3 is for reception.

As shown in Figure 9, Pin 1 of Port C is used for the motor drive circuit while Pin 1 of Port A is used for the pressure sensor.

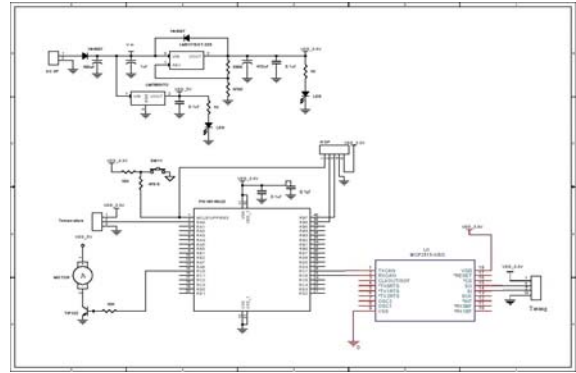


Figure 9. The D.C. Motor Module

As shown in Figure 10, Pin 1 of Port C is connected to the servo motor while Pin 1 of Port A is connected to the temperature sensor.

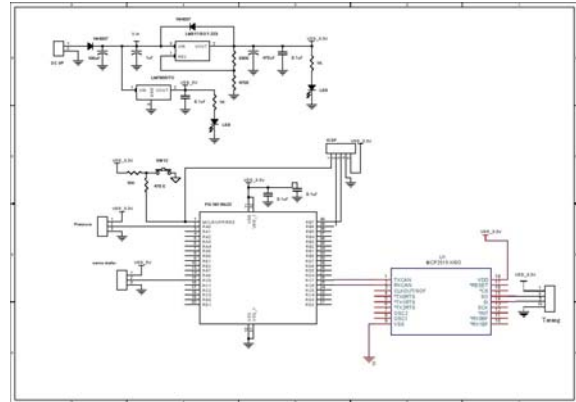


Figure 10. The Servo Motor Module

In Figure 11, the first three pins of Port A are connected to the Accelerator Sensor, Brake Sensor and Steering Sensor respectively.

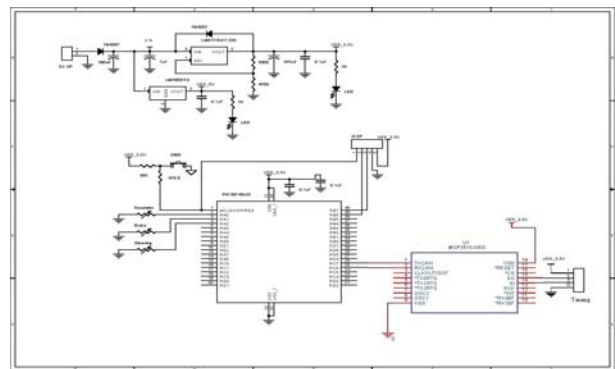


Figure 11. The Engine Control Module

## VI. ALGORITHM

Some of the pseudo-codes for various control units are shown below. MPLAB IDE is the development platform used for coding.

```
tostring(advalue1, dispstring);
cantx('A');
```



```

cantx(dispstring[0]);
cantx(dispstring[1]);
cantx(dispstring[2]);
cantx(dispstring[3]);
cantx(dispstring[4]);

```

In the above pseudo-code, the data obtained by various sensor units in the Engine Control Unit are converted into string and transmitted using CAN. Before transmission identification characteristics like 'A', 'B', etc are also transmitted.

```

if(adcvalue1 > adcvalue2)
    {
        accelerator = adcvalue1 - adcvalue2;
    }
else
    {
        accelerator = 0
    }

```

The above conditions are followed in the D.C. motor unit.

```

adcvalue1 = map(adcvalue1 , 0, 1023, 1, 150);
temp = adcvalue1;
angle1_act = temp;
angle11 = angle1_act/10;
datareceivedbit = 0;

```

The above condition is followed in the Servo motor unit. The ADC values obtained by the engine control module steering sensor is mapped as 1 for 0 and 150 for 1023 and the servo motor is driven.

## VII. HARDWARE OUTPUT

The Servo Motor Module is shown in Figure 12. It consists of a Servo Motor and a Level Sensor.

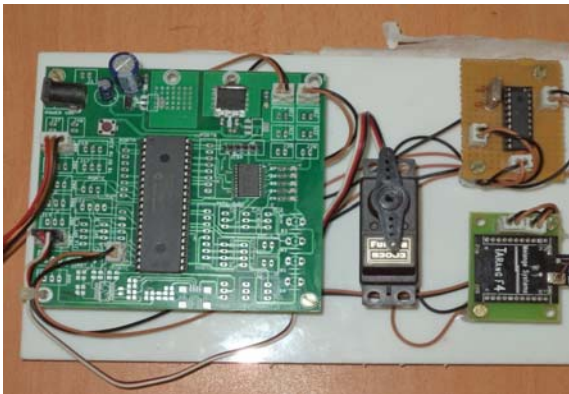


Figure 12. The Servo Motor Module

The Engine Control Module is shown in Figure 13. It consists of three sensors namely the accelerator sensor, the brake sensor and the steering sensor.

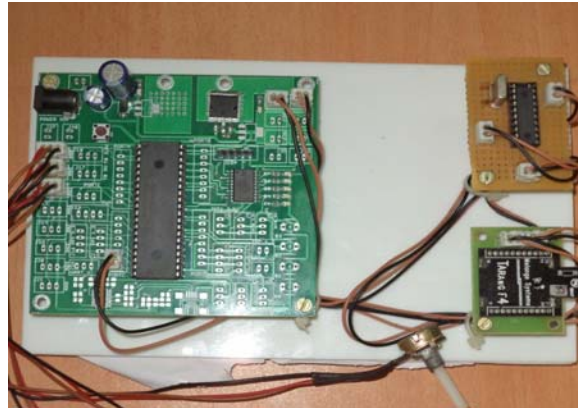


Figure 13. The Engine Control Module

The Dashboard Module is shown in Figure 14. It consists of a 16x2 LCD display.

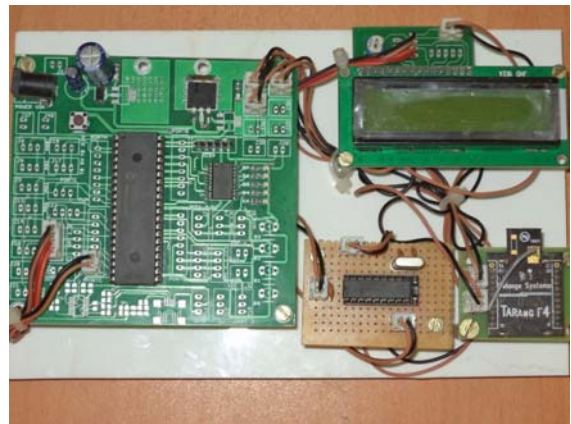


Figure 14. The Dashboard Module

The D.C. Motor Module is shown in Figure 15. It consists of a D.C. Motor and a Temperature Sensor.



Figure 15. The D.C. Motor Module

## VIII. CONCLUSION

With the above experiments, that the concept of drive-by-wireless is feasible. Error detection is also made easier using this technique. Safety of the automobile system is also guaranteed. Complexity, bulkiness and heaviness of the system is reduced. The system is also made less expensive.

## REFERENCES

- [1] Hauke St'ahle, Kai Huang, Alois Knoll, "Drive-by-Wireless with the eCar Demonstrator", Proceedings of the 4th ACM SIGBED International Workshop on Design, Modeling, and Evaluation of Cyber-Physical Systems. ACM, pp. 1-4, 2014.
- [2] Mary, Gerardine Immaculate, Zachariah C. Alex, and Lawrence Jenkins., "REAL TIME ANALYSIS OF WIRELESS CONTROLLER AREA NETWORK.", ICTACT JOURNAL ON COMMUNICATION TECHNOLOGY, Volume.05, Issue. 03, pp.951-958, September 2014.
- [3] J.-R. Lin, T. Talty, and O. Tonguz, "Feasibility of safety applications based on intra-car wireless sensor networks: A case study", in Vehicular Technology Conference (VTC Fall), 2011 IEEE, pp. 1-5, 2011.
- [4] C. Buckl, A. Camek, G. Kainz, C. Simon, L. Mercep, H. Staehle, and A. Knoll, "The software car: Building ict architectures for future electric vehicles", in Electric Vehicle Conference (IEVC), 2012 IEEE International, pp. 1-8, March 2012.
- [5] M. Eder and A. Knoll, "Design of an experimental platform for an x-by-wire car with four-wheel steering", in Automation Science and Engineering (CASE), 2010 IEEE Conference on, pp. 656-661, 2010.
- [6] Lin, Jiun-Ren, Timothy Talty, and Ozan K. Tonguz, "An empirical performance study of Intra-vehicular Wireless Sensor Networks under WiFi and Bluetooth interference", In Global Communications Conference (GLOBECOM), 2013 IEEE, pp. 581-586, 2013.
- [7] Torbitt, C., Tomsic, K., Venkataraman, J., Tsouri, G. R., Laifenfeld, M., & Dziatczak, M., "Investigation of waveguide effects in intra-vehicular environments", In Antennas and Propagation Society International Symposium (APSURSI), pp. 599-600, July, 2014.
- [8] Ahmed, Mohiuddin, Cem U. Saraydar, Tamer ElBatt, Jijun Yin, Timothy Talty, and Michael Ames, "Intra-vehicular wireless networks", In Globecom Workshops, 2007 IEEE, pp. 1-9, 2007.
- [9] Lin, Jiun-Ren, Timothy Talty, and Ozan K. Tonguz. "On the potential of bluetooth low energy technology for vehicular applications." Communications Magazine, IEEE, Vol.53, Issue. 1, pp. 267-275, 2015.
- [10] Iturri, Peio Lopez, Erik Aguirre, Leire Azpilicueta, Uxue Garate, and Francisco Falcone, "ZigBee Radio Channel Analysis in a Complex Vehicular Environment [Wireless Corner]", Antennas and Propagation Magazine, IEEE, Vol.56, no. 4, pp.232-245, 2014.
- [11] Deng, Han, Jia Li, Liuqing Yang, and Timothy Talty, "Intra-vehicle UWB MIMO channel capacity", In Wireless Communications and Networking Conference Workshops (WCNCW), 2012 IEEE, pp. 393-397, 2012.
- [12] Lu, Ning, Nan Cheng, Ning Zhang, X. S. Shen, and Jon W. Mark, "Connected Vehicles: Solutions and Challenges", pp. 1-1, 2014.
- [13] Firmansyah, Eka, and Lafiona Grezelda, "RSSI based analysis of Bluetooth implementation for intra-car sensor monitoring", In Information Technology and Electrical Engineering (ICITEE), 2014 6th International Conference on, pp. 1-5, 2014.
- [14] Salahuddin, Mohammad A., Ala Al-Fuqaha, and Mohsen Guizan, "Software Defined Networking for RSU Clouds in support of The Internet of Vehicles", 2012.
- [15] Gerla, Mario, Eun-Kyu Lee, Giovanni Pau, and Uichin Lee, "Internet of vehicles: From intelligent grid to autonomous cars and vehicular clouds", InInternet of Things (WF-IoT), 2014 IEEE World Forum on, pp. 241-246. IEEE, 2014.



**Gerardine Immaculate Mary** received her M.Tech degree with specialization in Wireless Communication from Pondicherry Engineering College, Pondicherry. She is now Assistant Professor (Selection Grade), School of Electronics Engineering, Vellore Institute of Technology (VIT), Vellore.

She also has over 12 years of industrial experience as computer hardware engineer. Her research areas include wireless communication in automation and vehicular environments, indoor wireless positioning and Ultra Wide-Band Technology applications. She has published several research papers in international journals and conferences.



**S.Srinath** is currently studying final year B.Tech Electronic and Communication Engineering in VIT University, Vellore, India.



## International Journal of Innovative Research in Computer and Communication Engineering

(An ISO 3297: 2007 Certified Organization)

Vol. 2, Issue 6, June 2014

# Design of 4<sup>th</sup> Order Parallel Coupled Microstrip Bandpass Filter at Dual Frequencies of 1.8 GHz and 2.4 GHz for Wireless Application

S.Srinath

UG Student, Dept. Of ECE, Vellore Institute Of Technology, Vellore, Tamilnadu, India

**ABSTRACT:** Design of a parallel-coupled microstrip bandpass filter is presented in this paper. The aim of this paper is to present the design technique, parameter analysis, real prototype fabrication and measurement results at dual simulation frequencies of 1.8GHz and 2.4GHz. Half wavelength long resonators and admittance inverters are used to design the filter. The filter is simulated using AWR Microwave Office software (Advanced Wave Research).

**KEYWORDS:** Bandpass filter; Microstrip; 1.8 GHz & 2.4GHz; Parallel Coupled Line; Microwave Engineering; AWR Simulator.

### I.INTRODUCTION

The microwave filter is a two port network which used to control the frequency response by providing transmission at frequencies within the passband and attenuation in the stopband of a filter. Filters are an essential part of telecommunications and radar systems. Of its low-cost fabrication, easy integration and simple designing procedure, the parallel coupled-line/edge-coupled filters are widely used in microwave microstrip circuits with a required bandwidth up to 20 % of central frequency . A bandpass filter only passes the frequencies within a certain desired band and attenuates others signals whose frequencies are either below a lower cutoff frequency or above an upper cut-off frequency. The range of frequencies that a bandpass filter let's to pass through is referred as passband. A typical bandpass filter can be obtained by combining a low-pass filter and a high-pass filter or applying conventional low pass to bandpass transformation . The architecture demonstrated here is a coupled line type filter, since this is among the most practical and common filter types which can meet the stated specifications. In Coupled Transmission Lines, coupling between two transmission lines is introduced by their proximity to each other. Coupling effects may be undesirable, such as crosstalk in printed circuits, or they may be desirable, as in directional couplers where the objective is to transfer power from one line to the other . Another of their major use is using them in filtering the Microwave range frequencies.

The filter response will be based on the Chebychev transfer function. Chebychev type filters are popular for their high selectivity, i.e., they have a relatively fast signal cut off between pass and stop band. Filters operating in gigahertz frequency ranges rely on distributed transmission line structures to obtain the desired frequency response. Dimensions of the coupled transmission lines can be derived with published formula or minimal simulation software capability.

### II.RELATED WORK

This paper presents the design of a parallel-coupled microstrip bandpass. The design is based on the use of half wave long resonators and admittance inverters. The dual center frequencies of 1.8 GHz & 2.4GHz are selected, the bandwidth (BW) is about 5%, the minimum attenuation amounts to -30 dB and the pass-band ripple is obtained equal to 0.5 dB.The design technique, parameter analysis, real prototype fabrication and measurement results of a 4<sup>th</sup> order coupled line bandpass filter at a dual simulation frequencies of 1.8GHz & 2.4GHz is presented in this paper.

# International Journal of Innovative Research in Computer and Communication Engineering

(An ISO 3297: 2007 Certified Organization)

Vol. 2, Issue 6, June 2014

### III. THEORY

A general layout of a parallel coupled microstrip bandpass is shown in figure 3.1 . The filter structure consists of open circuited coupled microstrip lines . These coupled lines are quarter wavelength , ( $\lambda/4$ ) long and are equivalent to shunt resonant circuits. The coupling gaps correspond to the admittance inverters in the low-pass prototype circuit. Even- and odd- mode characteristic impedances of parallel-coupled half-wave resonators are computed using admittance inverters. These even- and odd- mode impedances are then used to compute physical dimensions of the filter. Now consider a bandpass filter composed of a cascade of  $N + 1$  coupled line sections, as shown in Figure 3.1. The sections are numbered from left to right, with the load on the right, but the filter can be reversed without affecting the response. Since each coupled line section has an equivalent circuit of the form, the equivalent circuit of the cascade is as shown in Figure 3.2.

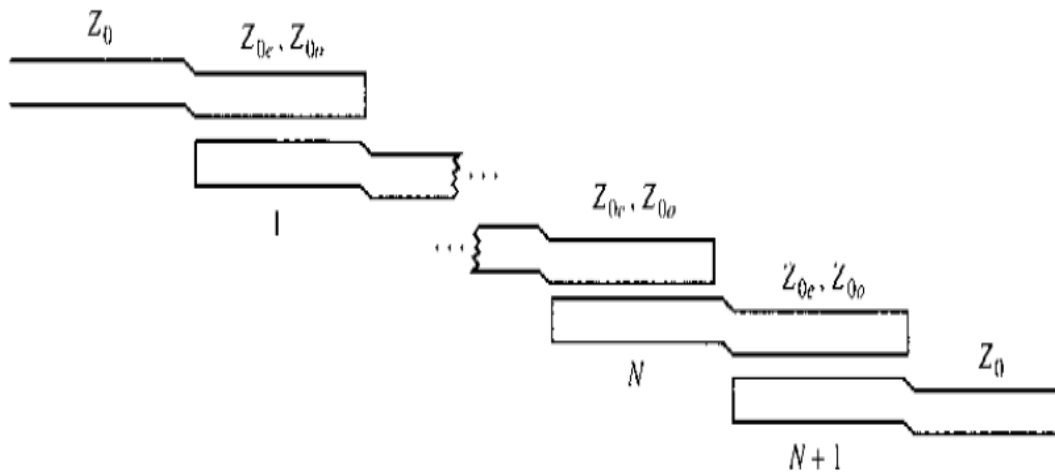


Figure 3.1 : Layout of an (N + 1)-section coupled line bandpass filter.

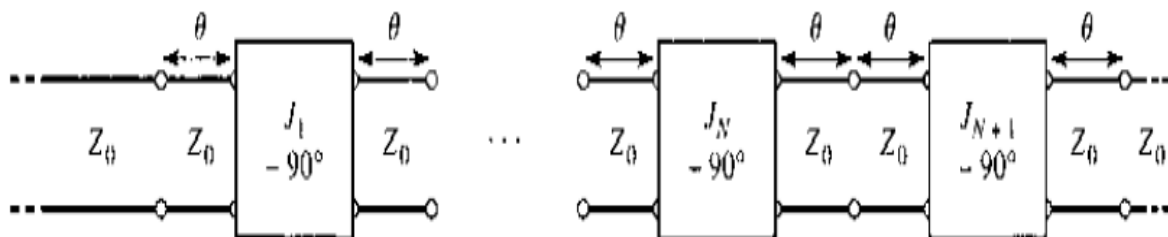


Figure 3.2 : Using the equivalent circuit of Figure 3.1 for each coupled line section.



# International Journal of Innovative Research in Computer and Communication Engineering

(An ISO 3297: 2007 Certified Organization)

Vol. 2, Issue 6, June 2014

## IV. IMMITTANCE INVERTER

Immittance inverters play a very important role in filter design. They are used to transform a filter circuit into an equivalent form that can be easily implemented using various microwave structures. Immittance inverters are either impedance or admittance inverters. Making use of the properties of immittance inverters, bandpass filters may be realized by series (L-C) resonant circuits separated by impedance inverters (K) or shunt (L-C) parallel resonant circuits separated by admittance inverters (J). To design a bandpass filter, first of all a low-pass prototype circuit is modified to include immittance inverters. These low pass structures are then converted to bandpass circuits by applying conventional low-pass to bandpass transformation.

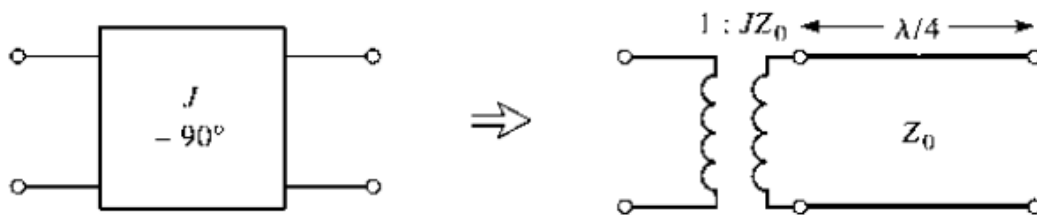


Figure 4.1 : Equivalent circuit of the admittance inverters.

## V. SIMULATION MODELING AND DISCUSSION

The design equations for the coupled line are as follows:

The order of the filter was calculated assuming an equi-ripple (Chebyshev type 1) response with an insertion loss (L) of 30dB at the center frequency of 1.8GHz and 2.4GHz and the passband ripple amplitude (G) of 0.5dB. The fractional bandwidth  $\Delta = 5\%$ .

Hence the upper and lower cutoff frequencies of the passband are 2.52 GHz and 2.28 GHz respectively. Using the standard Chebyshev model:

$$n = \frac{\cosh^{-1} \sqrt{(10^{\frac{L}{10}} - 1) / (10^{\frac{G}{10}} - 1)}}{\cosh^{-1} \left( \frac{f}{f_c} \right)}$$

This gives us  $n = 4$ . Now, we get the lowpass prototype values from the standard Chebyshev table:

$g_0 = 1$
$g_1 = 1.6704$
$g_2 = 2.3662$
$g_3 = 0.8419$
$g_4 = 1.9841$
$g_5 = 1.6704$

Now, we use the following design equations to get the inverter constants for a coupled line filter with  $N+1$  sections:

$$Z_0 J_1 = \frac{\sqrt{\Pi \Delta}}{\sqrt{2g_1}}$$

$$Z_0 J_n = \frac{\Pi \Delta}{2\sqrt{g_{n-1} g_n}} \quad ; n = 2, 3, 4 \dots N$$

# International Journal of Innovative Research in Computer and Communication Engineering

(An ISO 3297: 2007 Certified Organization)

Vol. 2, Issue 6, June 2014

$$Z_0 J_{n+1} = \sqrt{\frac{\Delta \Pi}{2g_n g_{n+1}}}$$

Using these equations, we get:

$Z_0 J_1 = 0.2168$
$Z_0 J_2 = 0.0556$
$Z_0 J_3 = 0.0467$
$Z_0 J_4 = 0.0556$
$Z_0 J_5 = 0.2168$

Now, the even and odd mode impedances can be calculated as follows:

$$Z_{oe} = Z_0 [1 + JZ_0 + (JZ_0)^2]$$

$$Z_{oo} = Z_0 [1 - JZ_0 + (JZ_0)^2]$$

The results of these calculations are tabulated below:

N	$Z_{oe}(\Omega)$	$Z_{oo}(\Omega)$
1	63.191	41.512
2	52.934	47.378
3	52.446	47.778
4	52.936	47.377
5	63.192	41.514

The substrate used is a standard FR4 substrate (MSUB) with  $\epsilon_r = 4.4$ ,  $H = 1.58\text{mm}$ ,  $T = 0.036\text{mm}$  and  $T_{and} = 0.005$ . Using a coupled line calculator, the width, length and line spacing for each coupled line was calculated:

Line	W(mm)	L(mm)	S(mm)
1	2.70182	69.11613	0.794745
2	2.98623	68.10692	3.450721
3	3.0021	68.05937	3.948424
4	2.98624	68.10694	3.450725
5	2.70188	69.11616	0.794743

Based on the above values and taking standard port impedances as  $Z_0 = 50\Omega$ , the design was simulated.

# International Journal of Innovative Research in Computer and Communication Engineering

(An ISO 3297: 2007 Certified Organization)

Vol. 2, Issue 6, June 2014

## V.SIMULATION DESIGN, RESULTS & DISCUSSION

The design was simulated using AWR Design Environment (9.00.4847) and a response was generated. The coupled line design used for simulation was MCFIL which is a non-floating line. This is a coupled line model with the end effect included for the open ended line. One side of each coupled line is the ground plane.

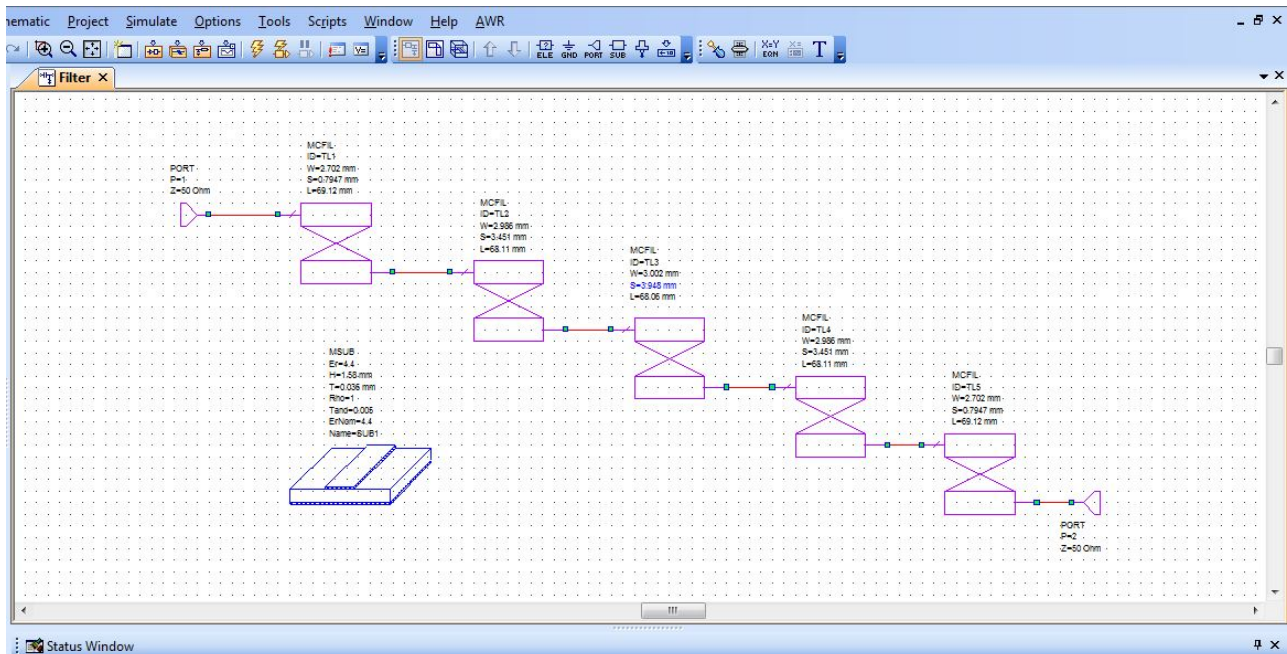


Figure 5.1 : Layout of the proposed 4<sup>th</sup> order filter design in AWR Software

Here, the parameter  $S_{11}$  (dB) represents the insertion loss at port 1 and this parameter which has a value of -6.521dB at the center frequency of 2.4 GHz while -6.587dB at the center frequency of 1.8GHz

The parameter  $S_{21}$  (dB) represents the insertion loss from port 1 to port 2 which has a value of -2.633dB at the center frequency of 2.4GHz while -6.375dB at the center frequency of 1.8GHz.

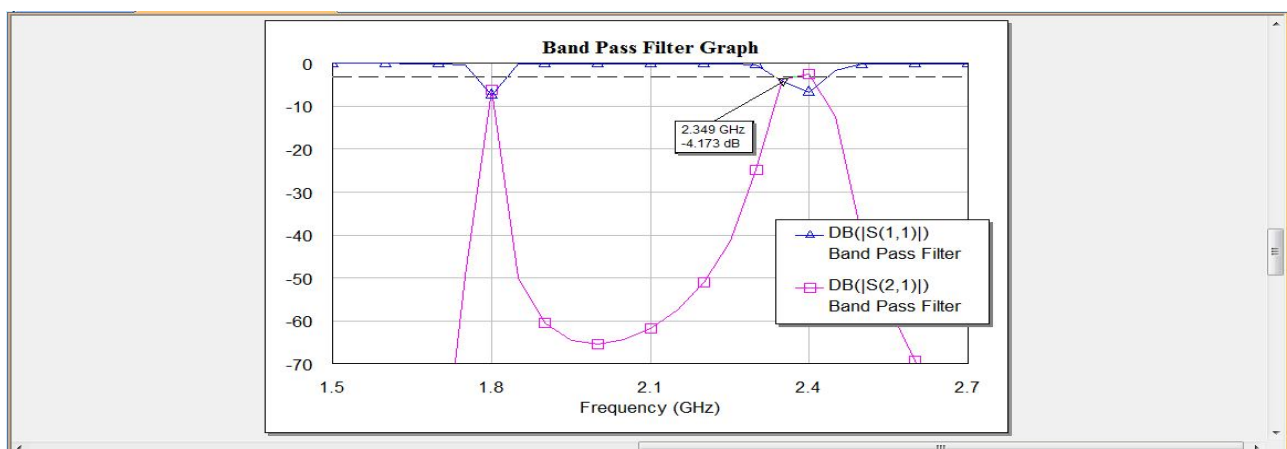


Figure 5.2 : Coupled Line Bandpass Filter at Dual Frequencies Result

The first design discussed above was simulated in AWR. The same was simulated using EM simulation. The schematic diagram for the same is given below:

# International Journal of Innovative Research in Computer and Communication Engineering

(An ISO 3297: 2007 Certified Organization)

Vol. 2, Issue 6, June 2014

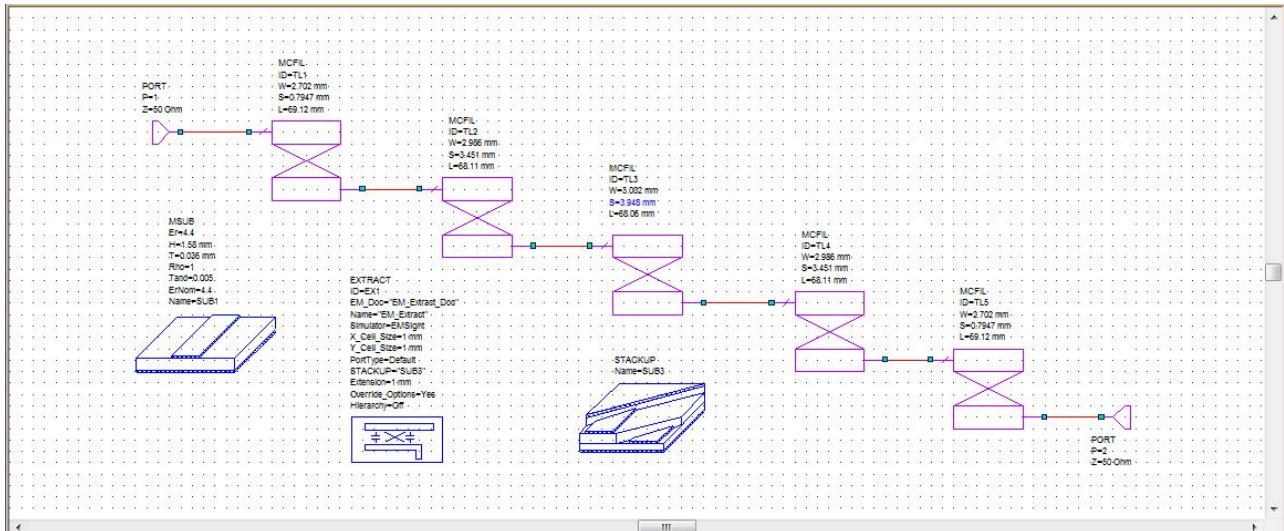


Figure 5.3 : Layout of the proposed 4<sup>th</sup> order filter design in AWR Software using EM simulation

Here, the parameter  $S_{11}$  (dB) represents the insertion loss at port 1 and the parameter which has a value of -2.606dB at the center frequency of 2.4 and 1.8GHz

The parameter  $S_{21}$  (dB) represents the insertion loss from port 1 to port 2 which has a value of -16.87dB at the center frequency of 2.4GHz while -31.55dB at the center frequency of 1.8GHz.

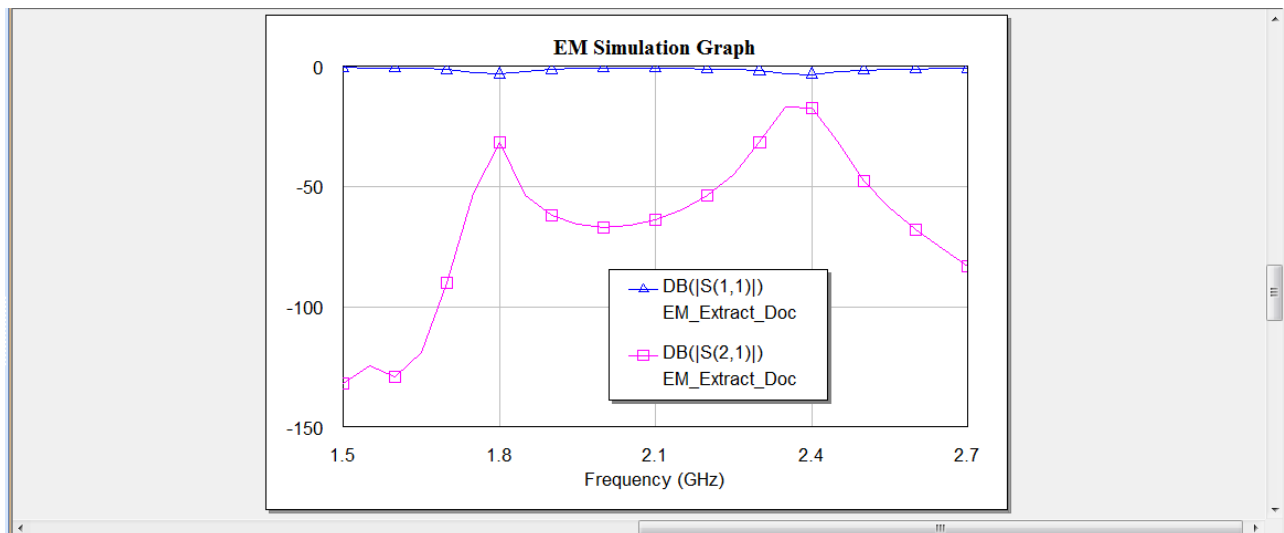


Figure 5.4 : Coupled Line Bandpass Filter at Dual Frequencies EM Simulation Result

For the Stackup, the dielectric used is FR4 and the conductor is copper. The transmission lines used in the design are MCLIN which are essentially similar to MCFIL lines with their remaining ends left open. The thickness of the dielectric layer is taken as 1.58mm and air thickness is taken as 24mm.

The simulation is done on EMSight with X and Y cell resolution of 0.5mm and an extension of 1mm. The extracted EM schematic is given below:



# International Journal of Innovative Research in Computer and Communication Engineering

(An ISO 3297: 2007 Certified Organization)

Vol. 2, Issue 6, June 2014

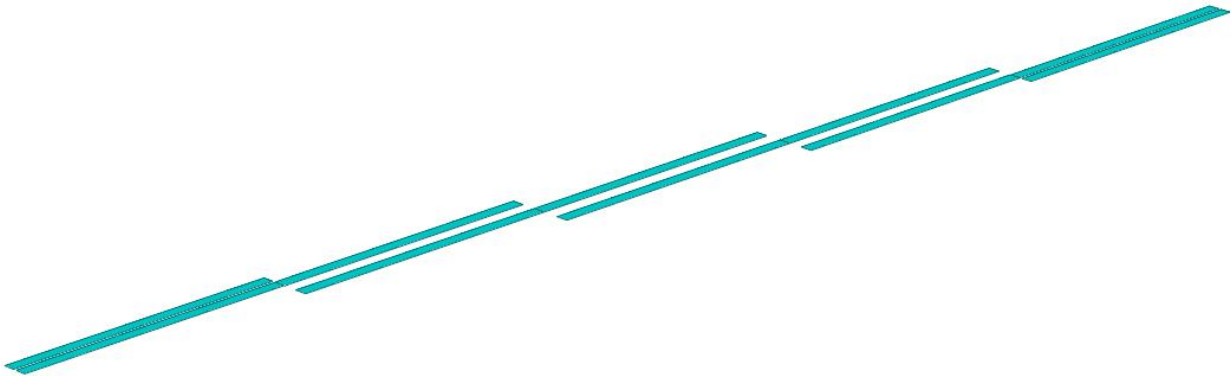


Figure 5.5 :3D View of the Coupled Line Bandpass Filter

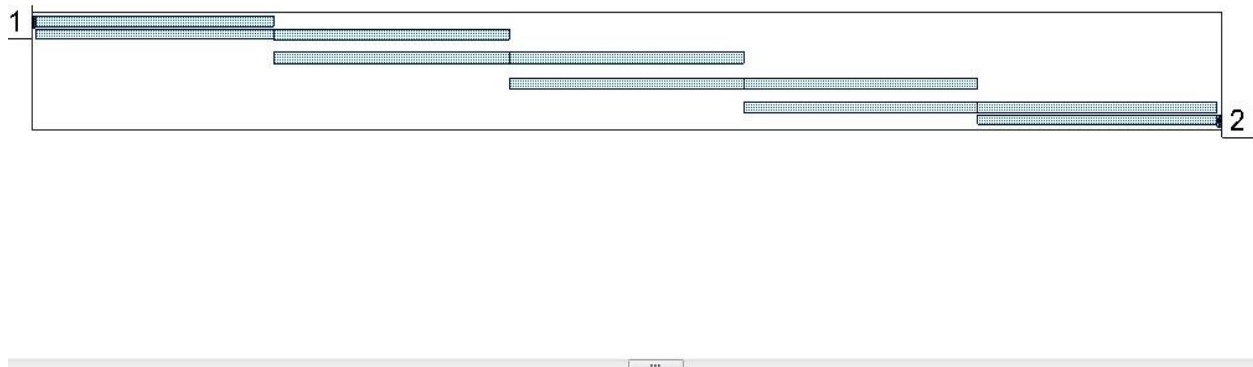


Figure 5.6 :3D View of the Extraced EM Strucure

## VI.CONCLUSION

On a substrate with a dielectric constant of 4.4, with the dual center frequencies of 1.8 GHz & 2.4 GHz, a coupled line bandpass filter was simulated with the bandwidth of about 5%, with the minimum attenuation of 30 dB and with the pass-band ripple equal to 0.5 dB. Thus the design technique, parameter analysis, real prototype fabrication and measurement results at dual simulation frequencies of 1.8GHz and 2.4GHz of a 4th order coupled line bandpass filter was presented in this paper.

## VIII.ACKNOWLEDGEMENT

At the outset, I would like to express my gratitude for my institute – Vellore Institute of Technology (V.I.T.) for providing me with the opportunity to undergo my undergraduate training, and assimilate knowledge and experience hitherto unknown to me.



# International Journal of Innovative Research in Computer and Communication Engineering

(An ISO 3297: 2007 Certified Organization)

Vol. 2, Issue 6, June 2014

## REFERENCES

- [1] D. M. Pozar, "Microwave Engineering", John Wiley & Sons Inc., 1998.
- [2] Miguel Bacaicoa, David Benito, Maria J. Garde, Mario Sorolla and Marco Guglielmi, "New Microstrip Wiggly-Line Filters with Spurious Pass-band Suppression", IEEE Transactions on microwave theory and techniques, vol. 49, no. 9, September 2001.
- [3] John T. Taylor and Qiuting Huang, "CRC Handbook of Electrical Filters", CRC Press, pp. 22-23, 1997.
- [4] "Tuning, Optimization and Statistical Design", Agilent Technologies, May 2003.  
R. Levy, S. B. Cohn, "A History of Microwave Filter Research, Design, and Development", Microwave Theory and Techniques, IEEE Transactions, vol. 32, no. 9, pp. 1055,1067, Sep 1984.
- [5] A. Naghar, O. Aghzout, F. Medina, M. Alaydrus, M. Essaidi, "Study and Design of a Compact Parallel Coupled Microstrip Band-Pass Filter for a 5 GHz Unlicensed Mobile WiMAX Networks," International Journal of Science and Technology, vol. 2, No. 6, June 2013.  
Sina Akhtarzard, Thomas R. Rowbotham, and Petter B. Johns, "The Design of Coupled Microstrip Lines", IEEE Transactions on Microwave Theory and Techniques, vol. MTT-23, no. 6, pp. 486-492, June 1975.  
E. O. Hammerstard, "Equations for microstrip circuit design," in Proceedings of the European Microwave Conference, Hamburg, Germany, 1975, pp. 268–272.
- [6] Annapurna Das and Sisir K Das, "Microwave Engineering", MacGraw Hill, p305, 2001.
- [7] Hong, J.S., M.J, "Microstrip Filter for RF/Microwave Applications", A Wiley- Interscience Publication, Canada, 2001.
- [8] C. A Balanis, "Antenna Theory: Analysis and Design", 3rd edition, Wiley, 2005.
- [9] S. B. Cohn, "Parallel-Coupled Transmission-Line-Resonator Filters," Microwave Theory and Techniques, IRE Transactions on , vol. 6, no. 2, pp. 223-231, April 1958.
- [10] S. Seghier, N. Benahmed, F. T. Bendimerad, N. Benabdallah, "Design of parallel coupled microstrip bandpass filter for FM Wireless applications", Sciences of Electronics, Technologies of Information and Telecommunications (SETIT), 6th International Conference , pp.207-211, 21-24 March 2012.  
A. R Othman, I.M. Ibrahim, M. F. M. Selamat, M. S. A. S. Samingan, A. A. A. Aziz, H. C. Halim, "5.75 GHz microstrip bandpass filter for ISM band", Applied Electromagnetics, APACE Asia-Pacific Conference on , pp. 1-5, 4-6 Dec. 2007.  
I. Azad, Md. A. H. Bhuiyan, S. M. Y. Mahbub, "Design and Performance Analysis of 2.45 GHz Microwave Bandpass Filter with Reduced Harmonics", International Journal of Engineering Research and Development, vol. 5, no. 11, pp. 57-67, 2013.
- [11] John T. Taylor and Qiuting Huang, "CRC Handbook of Electrical Filters", CRC Press, pp. 22-23, 1997.

## BIOGRAPHY



**S.SRINATH** passed 10<sup>th</sup> C.B.S.E. Board with a mark of 475/500(95%) and 12<sup>th</sup> C.B.S.E. Board from D.A.V. Boys Senior Secondary School, Gopalpuram, Chennai with a mark of 458/500(91.6%). Currently he is studying B.Tech, ECE, School of Electronics Engineering in VIT University, Vellore, India.

# Design and Real Prototype Fabrication Of a Free Space Optical Transmitter and Receiver

S.Srinath

UG Student, ECE, Vellore Institute of Technology, Vellore, India

**Abstract:** We are communicating with each others for every purpose. Different modes of communication are used. Free space optics is one of the mode of communication. Free space optics is widely used by satellites for transmitting with each other. Design and real prototype fabrication of a low cost portable free space optical transmitter and receiver is presented in this paper. Using this prototype wireless communication is possible. Light from a laser torch is used as the carrier in the circuit. The laser torch can transmit light up to a distance of about 500 meters. The transmitter circuit comprises of condenser microphone transistor amplifier BC548. The gain of the op-amp can be controlled with the help of 1-mega-ohm potmeter. The transmitter uses 9V power supply. The receiver circuit uses an npn phototransistor as the light sensor that is followed by a two-stage transistor preamplifier and LM386-based audio Power amplifier. This paper deals with the designing of a very low cost free space optical system which is perfect for information transmission of general conversation, using an ordinary available Laser torch of cost. The circuit is designed using National Instrumentations Multisim11.0 (**N.I. Multisim 11.0**) and National Instrumentations UltiBoard11.0 (**N.I. UltiBoard 11.0**).

**Keywords:** Battery driven design, Free space optics, Laser torch, Low cost design, N.I. Multisim and N.I. UltiBoard Simulator, Voice or data transmission.

## I. INTRODUCTION

This paper is based on the concept of Laser (Light Amplification by Stimulated Emission of Radiation) for transmitting analog as well as digital signals. As laser is stimulated radiation, problem of interference occurs in electromagnetic wave is eliminated, it can be a good substitution of present day communication systems and high deal of secrecy is available. Use of laser in communication systems is the future because of the advantages of the full channel speeds, no communication licenses required at present, compatibility with copper or fiber interfaces and no bridge or router requirements. Also it cannot be detected with use of spectrum analyzers and RF meters and hence can be used for diverse applications including financial, medical and military. Lasers can also transmit through glass. Laser transmitter and receiver units ensure easy, straightforward systems alignment and long-term stable, service free operation, especially in inaccessible environments. Optical wireless systems offer ideal, economical alternative to expensive leased lines for buildings. The laser can be commissioned in satellites for communication, as laser radar requires small aperture as compared to microwave radar. For voice transmission amplitude modulation of laser pulse was used to transmit the voice signal. Condenser microphone converts the voice into electric pulse which was then amplified and transmitted through laser. Photo detector at receiver detects the laser light and voice was output through loud speaker.

## II. RELATED WORK

This paper presents the design and real prototype fabrication of a free space optical system. The circuits are simulated in N.I. Multisim 11.0 and checked for validity and routing for the P.C.B. design is done with N.I. UltiBoard 11.0. The given design is thus checked and

routed as per 'INDUSTRY STANDARDS' and the real prototype can thus be etched out and a P.C.B. can be made on which components can be easily soldered. This paper mainly focuses on checking the validity of my design and performing a routing for my design for making a P.C.B.

## III. OBJECTIVES OF THE DESIGN

This paper aims to provide simple and cheap wireless communication design and real prototype fabrication for larger data rate with less distortion and to reduce the complexity for communication in the places where optical fiber or any wired communication is very difficult and expensive. The design is so easy, inexpensive and makeable with the available equipments that the technical as well as non technical person can construct it by themselves for their personal use.

### A. Block Diagram and Algorithm used for the Design

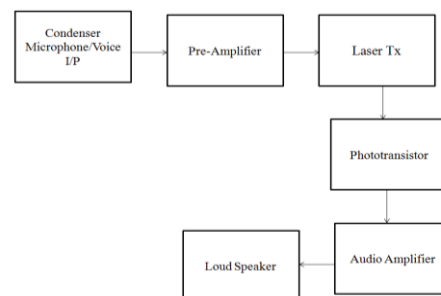
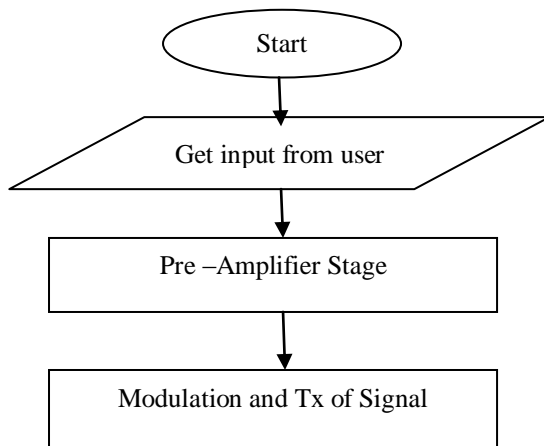


Fig. 1 Block Diagram for Voice and Data Transmission

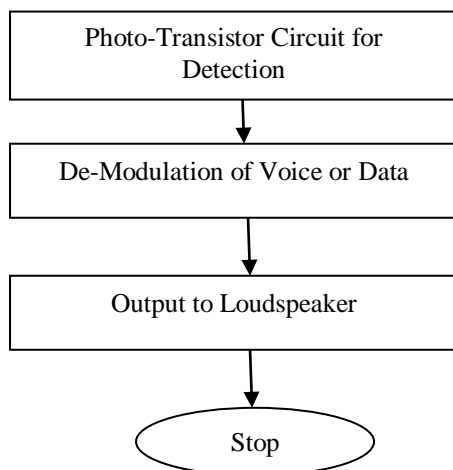
The algorithm is as follows. The input voice is taken through condenser microphone or a plug-in is taken as the input. The voice signal is amplified through the

preamplifier phase. Then, the signal is transmitted through laser light. The phototransistor at receiving side converts the signal into electrical signal. The electrical signal is passed through two transistor amplifier phases. Then LM386 audio amplifier amplifies the signal and drive speaker to generate voice output.

Flow Chart for Transmitter Circuit :



Flow Chart for Receiver Circuit :



#### IV. EQUIPMENTS REQUIRED

TABLE I  
EQUIPMENTS REQUIRED

Resistors All of (1/4W, 5% unless otherwise stated	Capacitors	Others
10R (brown, black, black) 1 Num	100 uF electrolytic 1Num	LM 358 IC 2Nos
100R (brown, black, brown) 2 Num.	10 uF electrolytic 3Nos.	LM 386 IC 1Num.
1K (brown, black, red) 1Num	100 nF monoblock (104) 4 Nos.	78L05 regulator 1Num

10K (brown, black, orange) 1Num	10 nF mylar (103) 2 Nos.	BC547 transistor 1 Num.
22K (red, red, orange) 2 Nos.	47nF box poly 1 Num	IF-D93 detector (red dot on black case) 1Num
100K (brown, black, yellow) 4Nos	-	IF-E96 emitter (pink dot on blue case) 1Num
220K (red, red, yellow) 1 Num.	-	Electret Microphone 1Num
680K (blue, grey, yellow) 1Num.	-	Speaker 8 ohm, 1W 1Num
1M (brown, black, green) 1Num.	-	8 pin DIL IC socket 3 Nos.
100K Koa trimpot (104) 1Num.	-	2 pole terminal block 3Nos.
-	-	9V battery snap 2Nos.

#### V. WORKING OF CIRCUIT DIAGRAM OF TRANSMITTER

The electret microphone converts sound waves to an electrical signal in the Tx circuit. R1 provides DC bias for the microphone and should be removed if you wish to connect any other input instead. This signal is coupled via C2 and amplified by two LM358 op amps, and converted to an optical signal by the LED emitter, driven from transistor Q1. R3 and R6 set the gain of IC1A to  $1+R3/R6$ , or 221. Since IC1A is direct coupled, R4/R2 determine the DC input and thus the DC output level. IC1B is also direct coupled and provides both the DC base current for Q1 and the AC modulation current. R7 determines the DC bias current for Q1. The modulated collector current drives the LED emitter.

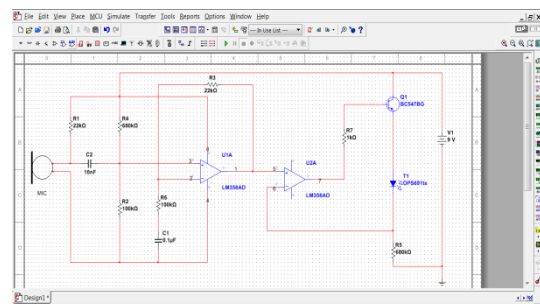


Fig. 2 Transmitter schematic in N.I. Multisim 11.0

#### VI. REAL PROTOTYPE FABRICATION OF TRANSMITTER

After checking the validity of the circuit in N.I. Multisim11.0, now convert the circuit to UltiBoard 11.0. To do this check if all the components are blue in colour(i.e. they have a foot-print) and select 'Transfer To UltiBoard 11.0' button.



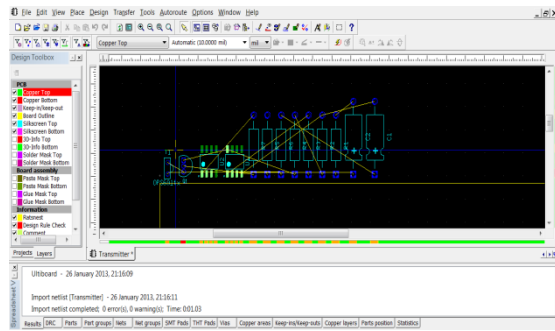


Fig. 3 Basic View of the Converted Schematic in N.I. UltiBoard 11.0

Now, align the components on the workspace and perform 'Routing'.

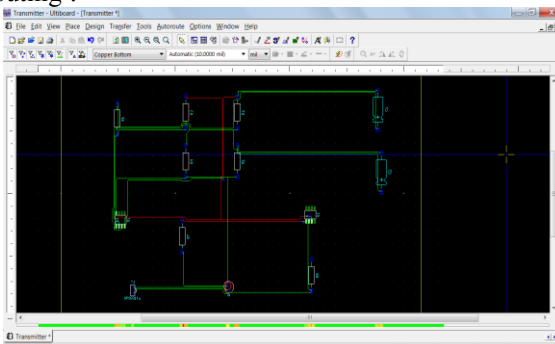


Fig. 4 View after Performing Routing of the Schematic in N.I. UltiBoard 11.0 for Transmitter Design

The 3D View of the real prototype fabrication of my design is shown below.

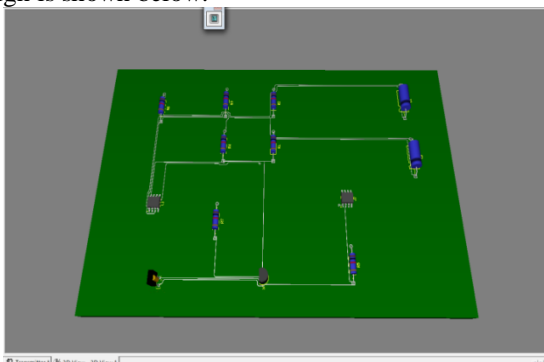


Fig. 5 3D View of my Design Showing PCB Connections for Transmitter Design

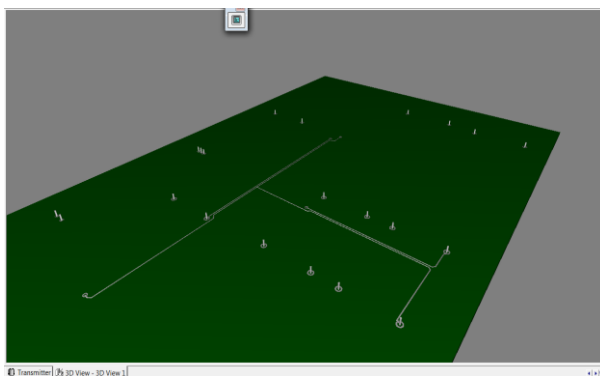


Fig. 6 3D View Showing Connections Appearing at the back-side of the PCB for Transmitter Design

## VII. WORKING OF CIRCUIT DIAGRAM OF RECEIVER

At the other end of the cable, the optical signal is directed at a photo-darlington detector in the receiver that converts it into an electrical signal again. The signal is amplified by op amp IC2 and power amp IC3 before being fed into a speaker where it becomes a sound wave. A voltage regulator has been used in the receiver gain stage to reduce DC supply ripple caused by the higher currents drawn in the power amplifier section. C1 and C2 are filter caps, C3 couples the detector voltage imposed across R1, into IC2. R2 and R4 set the op amp input to half the supply voltage, since only one supply is used rather than positive and negative supplies, as is usually the case. The gain of IC2 is adjustable by the pot in the feedback circuit. The range is therefore 1+1M/110k to 1+1M/10k, or 10 to 101. This is used as a volume control. IC2 output is coupled via C6 into an LM386 power amp IC with gain set to 20. R6 and C8 act as a low pass filter on the input. R7 and C9 form a network that provides a high frequency load to ensure stability.

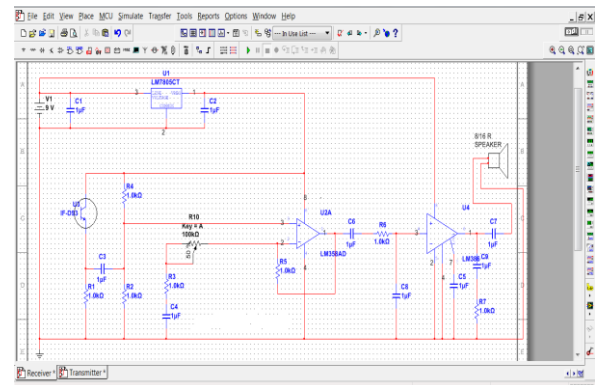


Fig. 7 Receiver schematic in N.I. Multisim 11.0

## VIII. REAL PROTOTYPE FABRICATION OF RECEIVER

After checking the validity of the circuit in N.I. Multisim11.0, now convert the circuit to UltiBoard 11.0. To do this check if all the components are blue in colour(i.e. they have a foot-print) and select 'Transfer To UltiBoard 11.0' button.

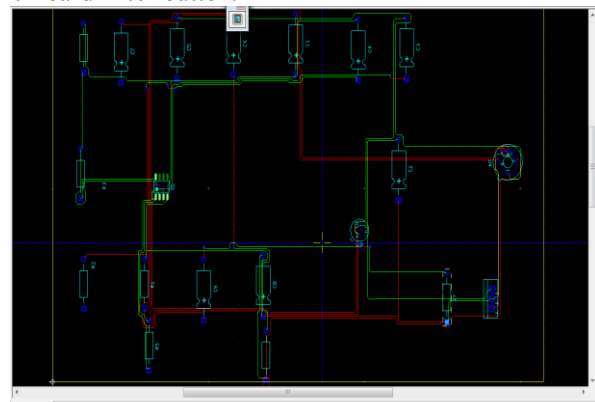


Fig. 8 View after Performing Routing of the Schematic in N.I. UltiBoard 11.0 for Receiver Design

The 3D View of the real prototype fabrication of my design is shown below.

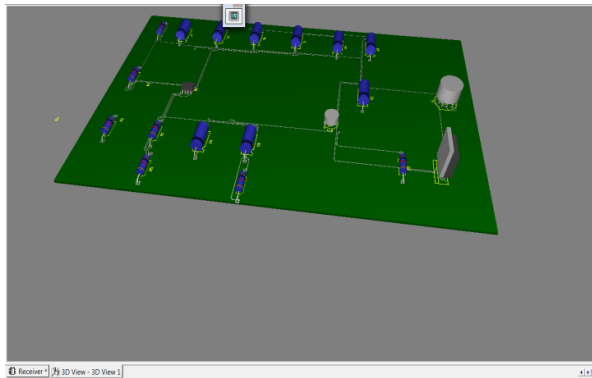


Fig. 9 3D View of my Design Showing PCB Connections for Receiver Design

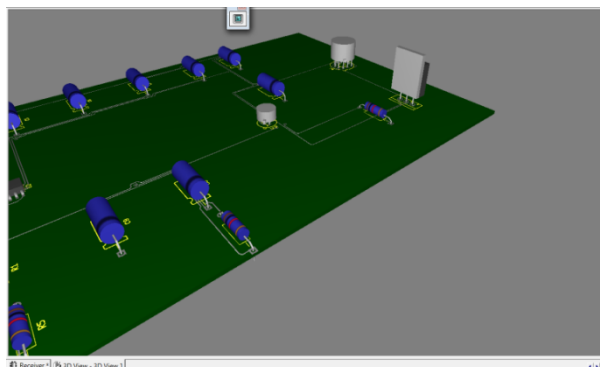


Fig. 10 3D Side View of my Design Showing PCB Connections for Receiver Design

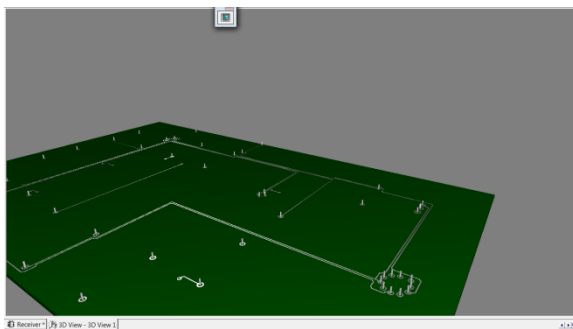


Fig. 11 3D View Showing Connections Appearing at the back-side of the PCB for Receiver Design

## IX. ADVANTAGES

Light from a laser torch is used as the carrier in the circuit instead of RF and FM signals. The laser transmission is very secure because it has a narrow beam[6]. The main advantage of this system is high reliability as it is impossible to track the data on the way of transmission. This design of Laser voice transmission system can be made at anywhere with low cost and can be used for frequent conversation at free of cost instead of using cell phone.

## X. CONCLUSION

This paper is completely based on wireless communication system. Presently there are various techniques which are being successfully used for transmission of data. The data transmission techniques employ RF, FM signals for transmission of data. Laser Torch Based Transmission

and Reception are cheaper and simpler in construction than RF transmitter and receiver. Although, wireless communication predominantly means the use of radio frequency for communication, the use of light based carriers for transfer of information is explored in this paper. This design can be made and used successfully at political assembly, lecture halls and for general conversation between two houses. The main problem with lasers is the beam dispersion can occurs due to external factors. In order to overcome these problems most advanced powerful lasers are to be employed. Although the optical data communication technology is prevailing from last decade as optical fiber communication devices available in the market, this design was presented to get all ideas that are behind such wireless system.

## ACKNOWLEDGMENT

At the outset, I would like to express my gratitude for my institute – Vellore Institute of Technology (V.I.T.) for providing me with the opportunity to undergo my undergraduate training, and assimilate knowledge and experience hitherto unknown to me.

## REFERENCES

- [1] I. Melngailis, "Laser development in Lincoln laboratory", The Lincoln Laboratory Journal, vol. 3, no. 3, pp. 347, 1990.
- [2] I. R. Sinclair and J. Dunton, "Practical Electronics Handbook", 6th ed. Oxford, U.K, Newnes, 2007, pp. 252-255.
- [3] Sedra, Adel.S and Smith, Kenneth C, "Microelectronic Circuits", Oxford University Press, 1998.
- [4] T. L. Floyd, "Electronic Devices", 6th ed. Singapore, Pearson Education, 2002, pp. 559-561.
- [5] C. M. M. Paschoal, D. Do N. Souza, and L. A. P. Santo, "Characterization of three photo detector types for computed tomography dosimetry", World Academy of Science, Engineering and Technology, no. 56, pp. 92-95, August 2011
- [6] "Laser and its applications," Popular Science & Technology Series, DRDO Publications, 2009.
- [7] O. Bishop, "Electronics Circuits and Systems", 4th ed. Oxford, U.K, Newnes, 2011, pp. 14.
- [8] I. R. Sinclair and J. Dunton, "Practical Electronics Handbook", 6th ed. Oxford, U.K, Newnes, 2007, pp. 252-255.
- [9] M. S. Islam and M. A. Rahman, "Design and fabrication of line follower robot," Asian Journal of Applied Science and Engineering, vol. 2, no. 2, pp. 27-32, 2013.
- [10] W. Tomasi, "Advanced Electronic Communication System", 6th ed.. New Jersey, U.S.A, Prentice-Hall, 2004, pp. 3, 41-42.
- [11] S. Gibilisco, "The Illustrated Dictionary of Electronics", 8th ed. New York, U.S.A, McGraw-Hill, 2001, pp. 399.
- [12] S. C. Singh, H. B. Zeng, C. L. Guo, and W. P. Cai, "Nanomaterials: Processing and Characterization with Lasers", 1sted. Wiley-VCH Verlag GmbH & Co. KGaA., 2012, ch. 1, pp.1.

## BIOGRAPHY



**S.SRINATH** passed 10<sup>th</sup> C.B.S.E. Board with a mark of 475/500(95%) and 12<sup>th</sup> C.B.S.E. Board from D.A.V. Boys Senior Secondary School, Gopalpuram, Chennai with a mark of 458/500(91.6%). Currently he is studying B.Tech, ECE, School of Electronics Engineering in VIT University, Vellore, India.

# Low Pass Filter Design Comparison Using Agilent Genesys

S.Srinath

Student, ECE, Vellore Institute of Technology, Vellore, India

**Abstract:** Wireless communication is becoming more and more popular. In this paper, a maximally flat low-pass filter and a equal-ripple low-pass filter have been designed for Ultra High Frequency (UHF) band ie I.T.U. band 9 (Frequency 300Mhz – 3000Mhz; Wavelength 1m – 100mm). Application of UHF band includes television, microwave ovens, mobile phones, wireless LAN, Bluetooth, etc. The filters are designed from the method of ‘Impedance and Frequency Scaling’. The design parameters and return loss are discussed. Also the amplitude (attenuation in dB) vs frequency graph is obtained for both the filters and their results are compared and suitable conclusions are drawn. The filters are designed using **Agilent Genesys 2010.05**

**Keywords:** Agilent Genesys Simulator; Low Pass Filter; Equal-ripple filter; Smith chart; Polar Chart; Maximally flat filter; Wireless communication; UHF Band Spectrum; S Parameters.

## I. INTRODUCTION

Various mobile cellular systems need a miniaturised size filter which should ideally have a sharp cut-off. Also, various radio frequency communication filters are gaining popularity. Low pass filters are widely preferred today. The need to filter out the transmitted and received signals with a specific bandwidth has been the task for many engineers today. Filter designs beyond 500MHz are difficult to realize with discrete components because the wavelength becomes comparable with the physical filter element dimensions, resulting in various losses severely degrading the circuit performance. Thus to arrive at practical filters, Impedance and Frequency Scaling is done and the lumped elements are directly simulated using RF simulator Agilent Genesys 2010.05.

In this paper, a maximally flat low-pass filter and a equal-ripple low-pass filter have been designed for Ultra High Frequency (UHF) band with a cutoff frequency of 700Mhz and order 7. A lumped L-C network is modelled with the ‘minimum inductor’ and ‘minimum capacitor’ configurations after Impedance and Frequency Scaling. Then, the amplitude (attenuation in dB) vs frequency plot is compared between the two filters. RF synthesis software ‘Agilent Genesys 2010.05’ is used for the purpose.



Agilent Genesys 2010.05 is an affordable, accurate, easy-to-use RF and microwave simulation software created for the circuit board and subsystem designer. It’s key features includes RF system analysis and frequency planning with interactive root-cause problem identification and linear and nonlinear RF circuit simulators with optimization and statistical analysis for high-performance and high-yield designs.

## II. RELATED WORK

In this paper, a maximally flat low-pass filter and a equal-ripple low-pass filter have been designed for Ultra High Frequency (UHF) band with a cutoff frequency of 700Mhz and order 7. The filters have input and output

resistances of 50 ohms. The filters are designed from the method of ‘Impedance and Frequency Scaling’. The design parameters and return loss are discussed. Also the amplitude (attenuation in dB) vs frequency graph is obtained for both the filters and their results are compared and suitable conclusions are drawn. The filters are designed using Agilent Genesys 2010.05

## III. THEORY [6]

For a normalized low-pass design, where the source impedance is  $1 \Omega$  and the cutoff frequency is  $\omega c = 1$  rad/sec, the element values for the ladder-type circuits in the below figures can be tabulated by using the standards tables.

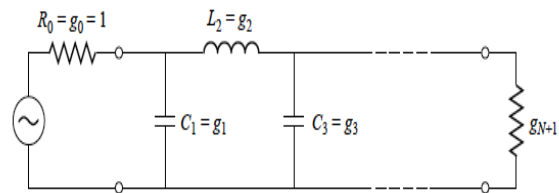


Fig.1. Ladder circuits for low-pass filter prototypes - Prototype beginning with a shunt element.

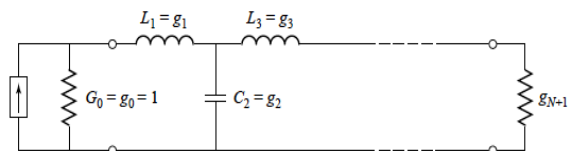


Fig.2. Ladder circuits for low-pass filter prototypes - Prototype beginning with a series element.

## IV. IMPEDANCE SCALING [6]

In the prototype design, the source and load resistances are unity . A source resistance of  $R_0$  can be obtained by multiplying all the impedances of the prototype design by  $R_0$ . Thus, if we let primes denote impedance scaled quantities, the new filter component values are given by

$$L' = R_0 L;$$

$$C' = \frac{C}{R_0};$$

$$R'_S = R_0;$$

$$R'_L = R_0 R_L;$$

where  $L$ ,  $C$ , and  $R_L$  are the component values for the original prototype.

### V. FREQUENCY SCALING [6]

To change the cutoff frequency of a low-pass prototype from unity to  $\omega c$  requires that we scale the frequency dependence of the filter by the factor  $\frac{1}{\omega c}$ , which is accomplished by replacing  $\omega$  by  $\frac{\omega}{\omega c}$ :

$$\omega \leftarrow \frac{\omega}{\omega c}$$

Then the new power loss ratio will be

$$P'_{LR}(\omega) = P_{LR}\left(\frac{\omega}{\omega c}\right);$$

where  $\omega c$  is the new cutoff frequency; cutoff occurs when  $\frac{\omega}{\omega c} = 1$ , or  $\omega = \omega c$ . This transformation can be viewed as a stretching, or expansion, of the original passband. The new element values are determined by applying the substitution of  $\omega \leftarrow \frac{\omega}{\omega c}$  to the series reactances,  $j\omega L_k$ , and shunt susceptances,  $j\omega C_k$ , of the prototype filter. Thus,

$$j X_k = j \left(\frac{\omega}{\omega c}\right) L_k = j \omega L'_k,$$

$$j B_k = j \left(\frac{\omega}{\omega c}\right) C_k = j \omega C'_k,$$

which shows that the new element values are given by

$$L'_k = \frac{L_k}{\omega c}$$

$$C'_k = \frac{C_k}{\omega c}$$

When both impedance and frequency scaling are required, the results of both Impedance and Frequency Scaling can be combined to give

$$(1.) \quad L'_k = \frac{R_0 L_k}{\omega c}$$

$$(2.) \quad C'_k = \frac{C_k}{R_0 \omega c}$$

### VI. CALCULATIONS AND DISCUSSION FOR BUTTERWORTH FILTER

First we find the order of the maximally flat filter to satisfy the insertion loss of 30 dB specification at 1200 MHz. We have that by  $|\omega/\omega c| - 1$  and from attenuation versus normalized frequency for maximum flat filter prototypes, we find the order to be  $N=7$ .

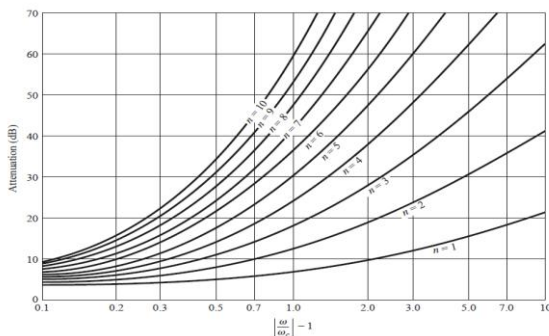


Fig.3. Attenuation versus normalized frequency for maximally flat filter prototypes.

Order									
1	1	2	1						
2	1	1.41421	1.41421	1					
3	1	1	2	1	1				
4	1	0.765367	1.84776	1.84776	0.765367	1			
5	1	0.618034	1.61803	2	1.61803	0.618034	1		
6	1	0.517638	1.41421	1.93185	1.93185	1.41421	0.517638	1	
7	1	0.445042	1.24698	1.80194	2	1.80194	1.24698	0.445042	1

Fig.4. Element Values for Maximally Flat LowPass Filter Prototypes.

Now, we get the lowpass prototype values from the standard Butterworth table given above:

$g_1 = 0.445042$
$g_2 = 1.24698$
$g_3 = 1.80194$
$g_4 = 2$
$g_5 = 1.80194$
$g_6 = 1.24698$
$g_7 = 0.445042$

Then Impedance and Frequency Scaling method {(1.) and (2.)} can be used to obtain the scaled element values for 'minimum inductor' type as : (Here :  $R_0 = 50$  Ohms ;  $f_c = 700$ Mhz )

$C'_1 = 2.023$ pF
$L'_1 = 14.175$ nH
$C'_2 = 8.193$ pF
$L'_2 = 22.736$ nH
$C'_3 = 8.193$ pF
$L'_3 = 14.175$ nH
$C'_4 = 2.023$ pF

Similarly, the Impedance and Frequency Scaling method {(1.) and (2.)} can be used to obtain the scaled element values for 'minimum capacitor' type as : (Here :  $R_0 = 50$  Ohms ;  $f_c = 700$ Mhz )

$L'_1 = 5.059$ nH
$C'_1 = 5.670$ pF
$L'_2 = 20.484$ nH
$C'_2 = 9.094$ pF
$L'_3 = 20.484$ nH
$C'_3 = 5.670$ pF
$L'_4 = 5.059$ nH



### VII. CALCULATIONS AND DISCUSSION FOR EQUI- RIPPLE FILTER

Here too, we first find the order of the maximally flat filter to satisfy the insertion loss of 35 dB specification at 1000 MHz and a passband ripple of 0.25dB. We have that by  $|\omega/\omega_c| - 1$  and from attenuation versus normalized frequency for equi-ripple filter prototypes, we find the order to be N=7.

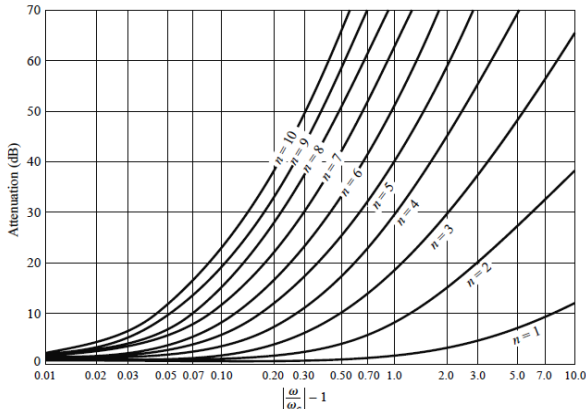


Fig. 5. Example of an attenuation versus normalized frequency for equal-ripple filter prototypes with 0.5 dB ripple level ( In this paper 0.25 dB ripple level plot is considered and the order thus calculated is 7).

The order can also be found out by using the equation the standard Chebyshev model

$$n = \frac{\cosh^{-1} \sqrt{(10^{\frac{L}{10}} - 1)/(10^{\frac{G}{10}} - 1)}}{\cosh^{-1}(\frac{f}{f_c})}$$

Order									
1	1	0.486867	1						
2	1	1.1132	0.687327	1.61961					
3	1	1.30344	1.14628	1.30344	1				
4	1	1.37824	1.26933	2.05581	0.850972	1.61961			
5	1	1.41446	1.318	2.24141	1.318	1.41446	1		
6	1	1.43458	1.34217	2.3126	1.42788	2.17378	0.885758	1.61961	
7	1	1.44686	1.35597	2.34759	1.4689	2.34759	1.35597	1.44686	1

Fig.6. Standard Chebyshev table with passband ripple of 0.25dB.

Now, we get the lowpass prototype values from the standard Chebyshev table given above:

$g_1 = 1.44686$
$g_2 = 1.35597$
$g_3 = 2.34759$
$g_4 = 1.4689$
$g_5 = 2.34759$
$g_6 = 1.35597$
$g_7 = 1.44686$

Then Impedance and Frequency Scaling method {(1.) and (2.)} can be used to obtain the scaled element values for

'minimum inductor' type as : (Here : R0 = 50 Ohms ; fc = 700Mhz )

$C'_1 = 6.579\text{pF}$
$L'_1 = 15.415\text{nH}$
$C'_2 = 10.675\text{pF}$
$L'_2 = 16.699\text{nH}$
$C'_3 = 10.675\text{pF}$
$L'_3 = 15.415\text{nH}$
$C'_4 = 6.579\text{pF}$

Similarly, the Impedance and Frequency Scaling method {(1.) and (2.)} can be used to obtain the scaled element values for 'minimum capacitor' type as : (Here : R0 = 50 Ohms ; fc = 700Mhz )

$L'_1 = 16.448\text{nH}$
$C'_1 = 6.166\text{pF}$
$L'_2 = 26.688\text{nH}$
$C'_2 = 6.679\text{pF}$
$L'_3 = 26.688\text{nH}$
$C'_3 = 6.166\text{pF}$
$L'_4 = 16.448\text{nH}$

### VIII. SIMULATION DESIGN, RESULTS AND DISCUSSION FOR BUTTERWORTH FILTER

The design was simulated using Agilent Genesys 2010.05 and a response was generated. The filter is a lowpass Butter worth filter with input resistance = 50 ohm, cutoff frequency = 700 MHz and Order = 7.

The Minimum Inductor type 7<sup>th</sup> order filter layout is shown below.

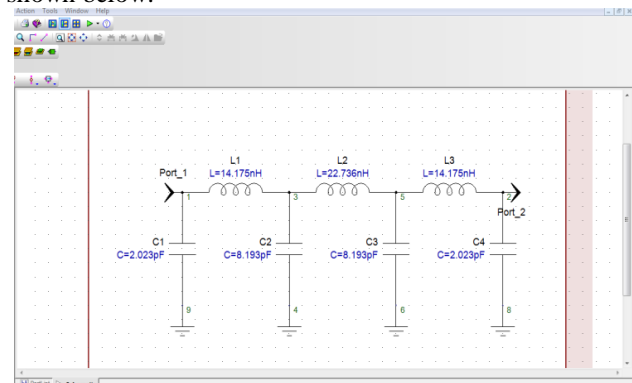


Fig.7. Minimum Inductor type 7<sup>th</sup> order filter layout.

The result is generated, with parameter values which meet the requirements. A plot of S21 and S11 are produced.

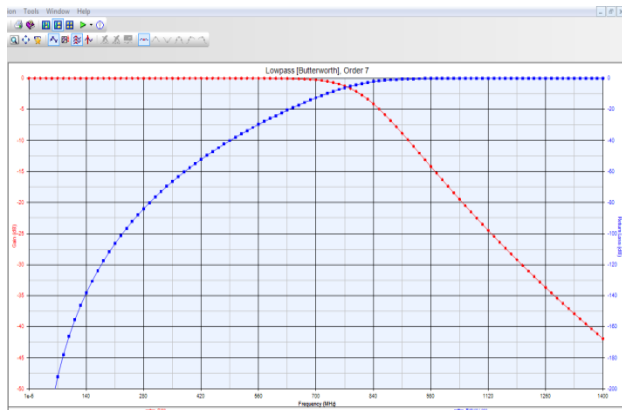


Fig. 8. The amplitude (attenuation in dB) vs frequency results for the 7<sup>th</sup> order minimum Inductor type filter.

The required results were obtained for the minimum capacitor type filter. A plot of S21 and S11 are produced.

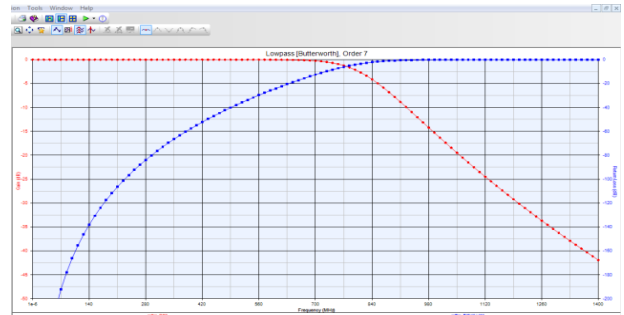


Fig.12. The amplitude (attenuation in dB) vs frequency results for the 7<sup>th</sup> order minimum Capacitor type filter.

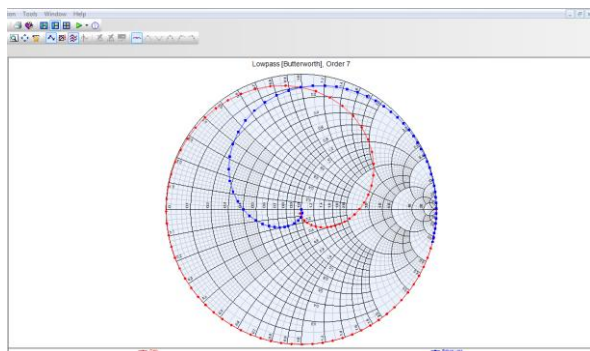


Fig.9. Gain and return loss on a smith chart of the filter .

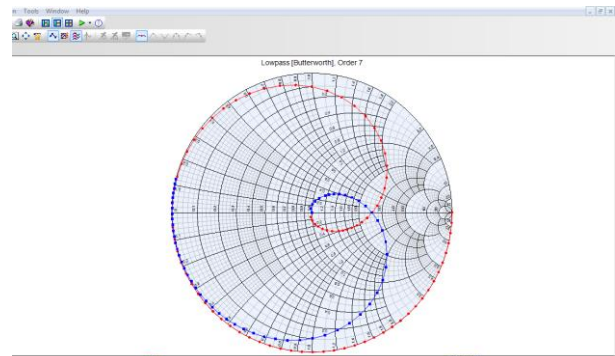


Fig.13. Gain and return loss on a smith chart of the filter.

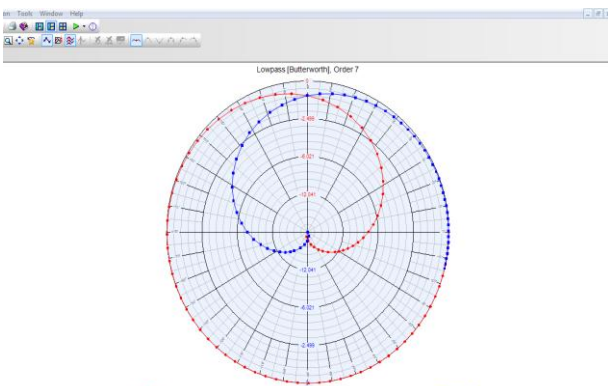


Fig.10. Gain and return loss on a polar chart of the filter .

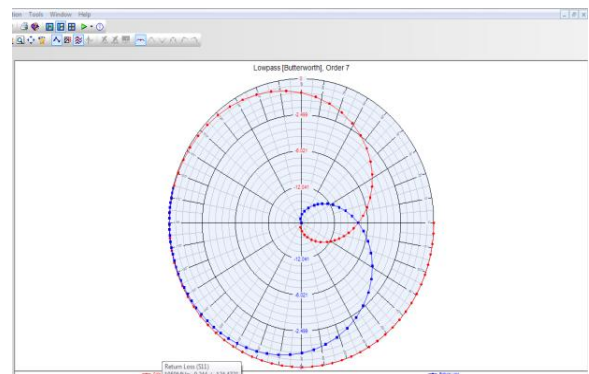


Fig.14. Gain and return loss on a polar chart of the filter.

The Minimum Capacitor type 7<sup>th</sup> order filter layout is shown below.

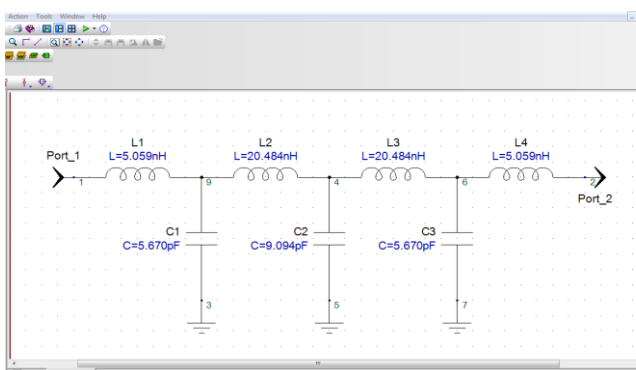


Fig.11. Minimum Capacitor type 7<sup>th</sup> order filter layout.

### IX. SIMULATION DESIGN, RESULTS AND DISCUSSION FOR CHEBYSHEV FILTER

The design was simulated using Agilent Genesys 2010.05 and a response was generated. The filter is a lowpass Chebyshev filter with input resistance = 50 ohm, cutoff frequency = 700 MHz and Order = 7.

The Minimum Inductor type 7<sup>th</sup> order filter layout is shown below.

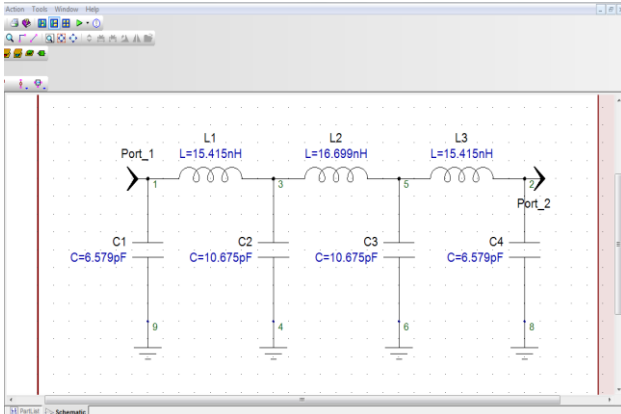


Fig.15. Minimum Inductor type 7<sup>th</sup> order filter layout.

The result is generated, with parameter values which meet the requirements. A plot of S21 and S11 are produced.

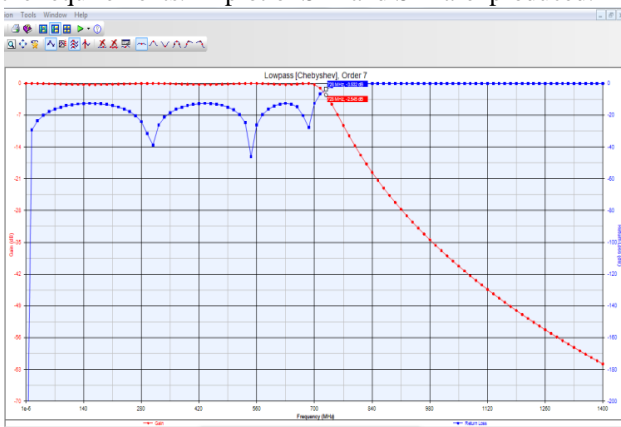


Fig.16. The amplitude (attenuation in dB) vs frequency results for the 7<sup>th</sup> order minimum inductor type filter.

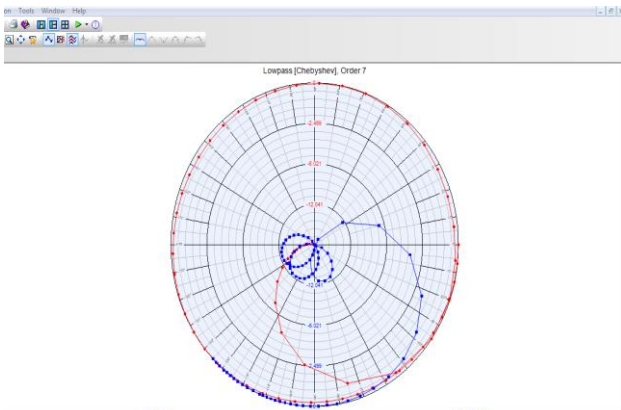


Fig.17. Gain and return loss on a polar chart of the filter .

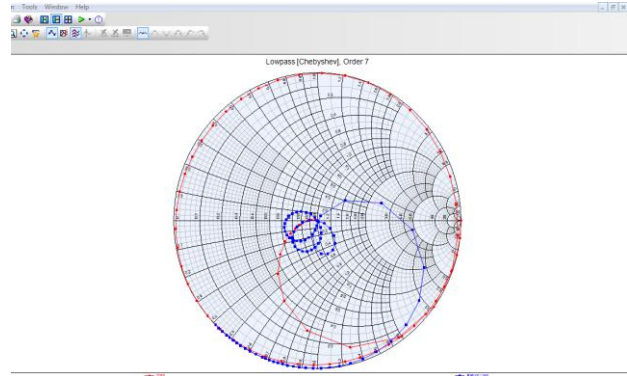


Fig.18. Gain and return loss on a Smith chart of the filter.

The Minimum Capacitor type 7<sup>th</sup> order filter layout is shown below.

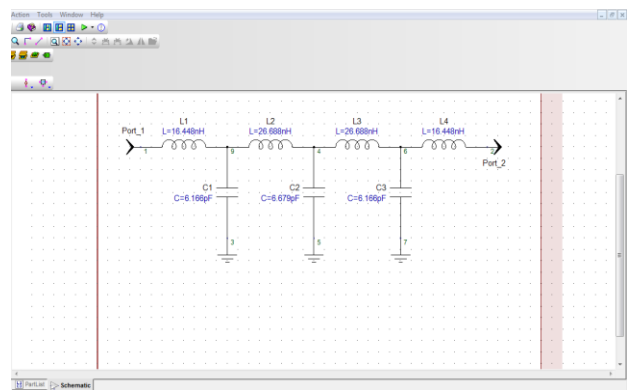


Fig.19. Minimum Capacitor type 7<sup>th</sup> order filter layout.

The result is generated, with parameter values which meet the requirements. A plot of S21 and S11 are produced.

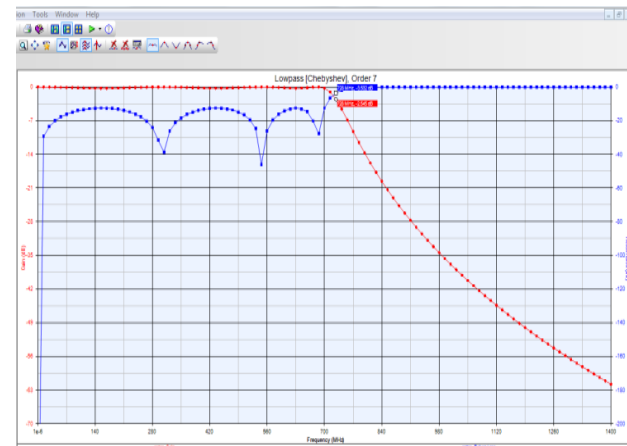


Fig. 20. The amplitude (attenuation in dB) vs frequency results for the 7<sup>th</sup> order minimum Capacitor type filter.

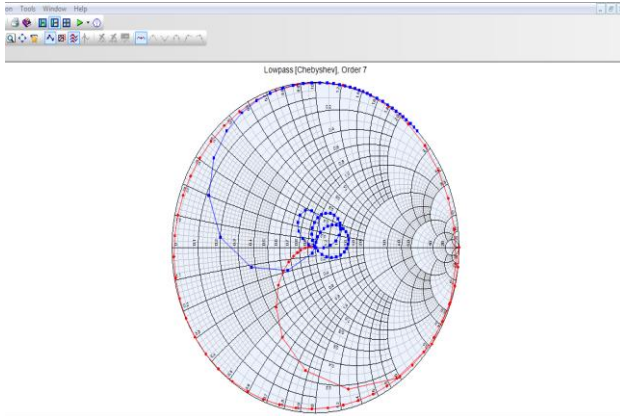


Fig.21. Gain and return loss on a Smith chart of the filter.

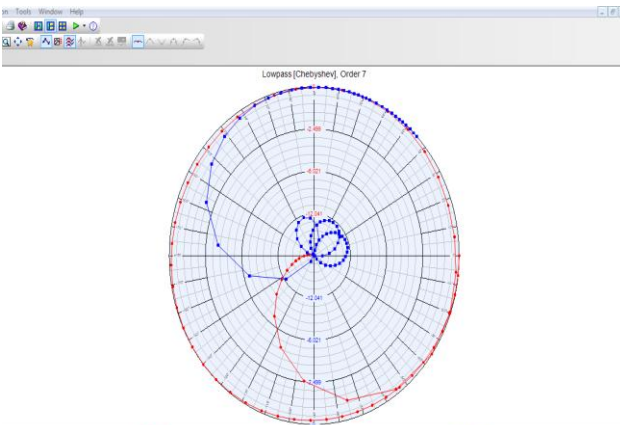


Fig.22. Gain and return loss on a polar chart of the filter

## X. CONCLUSION

This paper deals with the design of a maximally flat low-pass filter and a equal-ripple low-pass filter (pass band ripple = 0.25 dB ripple). Both the filters have a cutoff frequency of 700 MHz, input resistance of 50 ohms and an order of 7. The amplitude (attenuation in dB) vs frequency results for these filters are shown in the above figures. These results clearly show the trade-offs involved with the two types of filters. The equal-ripple response has the sharpest cutoff. The maximally flat response has a flatter attenuation characteristic in the passband but a slightly lower cutoff rate.

The measured 3 dB frequency is 818.99 MHz for butter worth filter and the measured 3 dB frequency for Chebyshev filter is 731.46 Mhz.

## ACKNOWLEDGMENT

At the outset, I would like to express my gratitude for my institute – Vellore Institute of Technology (V.I.T.) for providing me with the opportunity to undergo my undergraduate training, and assimilate knowledge and experience hitherto unknown to me.

## REFERENCES

- [1] J.C. Rautio, *Planar electromagnetic analysis*, IEEE Microwave Magazine, Vol. 4, No. 1, March 2003, pp. 35-41.
- [2] J.S. Hong, and M.J. Lancaster, *Microstrip Filters for RF/Microwave Applications*, Wiley, New York, 2001.

- [3] D. Ahn, J. S. Park, C.S. kim, J. Kim, Y. Qian, and T. Itoh., "Design of the Low-Pass Filter using the Novel Microstrip Defected Ground Structure", *IEEE Trans. Microwave Theory Tech*, Vol. 49, pp. 86-92, January.
- [4] E.H. Fooks and R.A. Jakarevicius, *Microwave Engineering using Microstrip Circuits*, Prentice Hall of Australia, pp. 167-169, 1990.
- [5] M. Makimoto, S. Yamashita, "Microwave Resonators and Filters", *IEEE Trans. Wireless communication* Vol. 2, August, 1986.
- [6] D.M. Pozar, *Microwave Engineering*, John Wiley, 2000.
- [7] R. Levy, R.V. Snyder and G. Matthaei, "Design of Microwave Filters", *IEEE Transactions On Microwave Theory*, vol. 50, pp. 783-793, March 2002.
- [8] Roman Kaszynski and Jacek Piskorowski, "New Concept of Delay-Equalized Low Pass Butterworth Filters," *IEEE Symposium on Industrial Electronics and Application (ISIEA 2009)*, vol. 1, pp. 171-175, 9-12 July, 2006.
- [9] Srinath, S. "Design and Electromagnetic Modeling of E-Plane Sectoral Horn Antenna For Ultra Wide Band Applications On WR-137 & WR-62 Waveguides.", *International Journal of Engineering and Science Invention*, Vol. 3, Issue. 7, pp: 11-17, July, 2014.
- [10] Li Zhongshen, "Design and Analysis of Improved Butterworth Low Pass Filter", *The Eighth International Conference on Electronic Measurements and Instruments*, pp. 1729-1732, 2007.
- [11] John T. Taylor and Qiuting Huang, *CRC Handbook of Electrical Filters*, CRC Press, pp. 22-23, 1997.
- [12] C. A. Balanis, *Antenna Theory: Analysis and Design*, 3rd edition, Wiley, 2005.
- [13] D. H. Werner and S. Ganguly, "Fractal Antenna Engineering Research," *IEEE Trans. Antennas Propagat.*, Vol. 45, No. 1, pp. 38-57, Feb 2003.
- [14] Ting, S. W., K. W. Tam, and R. P. Martins, "Miniaturized microstrip lowpass filter with wide stopband using double equilateral U-shaped defected ground structure," *IEEE Trans. Microw. Wireless Compon. Lett.*, Vol. 16, No. 5, May 2006.
- [15] Xiao, J.-K., Q.-X. Chu, and H.-F. Huang, "New microstrip lowpass filter with transmission zero and wide stopband," *2008 China-Japan Joint Microwave Conference*, Sep. 10-12, 2008.
- [16] Wuren, T., I. Sakagami, M. Fujii, and M. Tahara, "A miniaturized microstrip ring resonator lowpass filter with sharp attenuation," *2008 IEEE MTT-S International Microwave Symposium Digest*, Jun. 15, 2008.
- [17] Srinath, S. "Design of 4th Order Parallel Coupled Microstrip Bandpass Filter at Dual Frequencies of 1.8 GHz and 2.4 GHz for Wireless Application.", *International Journal of Innovative Research in Computer and Communication Engineering*, Vol. 2, Issue. 6, June, 2014.
- [18] S. S. Mohammed, K. Ramasamy, and T. Shanmuganatham, "Wireless power transmission - A next generation power transmission system," *International Journal of Computer Applications*, vol. 1, no. 13, pp. 100-103, 2010.
- [19] R. Ludwig and P. Bretchko, *RF Circuit Design - Theory and Application*, New Jersey, USA: Prentice-Hall, Inc., 2000.
- [20] P. K. Sharma, V. S. Jadun, D. K. Mahor, and A. Verma, "Designing microstrip low pass filter in ISM band for rectenna system," *International Journal of Engineering And Technology*, vol. 1, no. 4, 2012.
- [21] T. Moyra, S. K. Parui, and S. Das, "Design of a quasi-elliptic lowpass filter using a new defected ground structure and capacitively loaded microstrip line," *International Journal on Electrical Engineering and Informatics*, vol. 3, no. 11, 2011.
- [22] Chen, X.-Q., R. Li, S.-J. Shi, Q. Wang, L. Xu, and X.-W. Shi, "A novel low pass filter using elliptic shape defected ground structure", *Progress In Electromagnetics Research B*, Vol. 9, pp: 117-126, 2008.

## BIOGRAPHY



**S.SRINATH** passed 10<sup>th</sup> C.B.S.E. Board from Chinmaya Vidyalaya, Virugambakkam with a mark of 475/500(95%) and 12<sup>th</sup> C.B.S.E. Board from D.A.V. Boys Senior Secondary School, Gopalpuram, Chennai with a mark of 458/500(91.6%). Currently he is studying final year B.Tech, ECE, School of Electronics Engineering in VIT University, Vellore, India.





# **Optisystem based CATV System-Performance Improvement by Using External Light-Injection Technique**

S.Adithyan<sup>1</sup>, S.Srinath<sup>2</sup>

U.G. Student, Department of EEE, C. Abdul Hakeem College of Engineering & Technology, Vellore, Tamilnadu, India<sup>1</sup>

Final Year Student, B.Tech, Department of ECE, Vellore Institute of Technology, Vellore, Tamilnadu, India<sup>2</sup>

**ABSTRACT:** Cable Television (CATV) is designed with erbium-doped amplifier-repeated system that uses an external light – injection technique and a directly modulated wave using amplitude modulation. The external light – injection technique can greatly enhance the frequency response of the laser diode, and hence improve the overall performance of the fibre optical CATV system. It implemented using **Optiwave Optisystem 10.0**.

**KEYWORDS:** External Light-Injection Technique, Semiconductor Lasers, Optical Communication, Directly Modulated Transmitter.

## **I.INTRODUCTION**

CATV is a shared cable system that uses a tree-and-branch topology in which multiple households within a neighborhood share the same cable. Cable television is a system of distributing television programs to subscribers via radio frequency (RF) signals transmitted through coaxial cables or light pulses through fiber-optic cables. The abbreviation CATV is often used for cable television. It originally stood for Community Access Television or Community Antenna Television, from cable television's origins in 1948, in areas where over-the-air reception was limited by distance from transmitters or mountainous terrain, large "community antennas" were constructed, and cable was run from them to individual homes.

## **II.RELATED WORK**

Lu et al [7] developed a CATV system Based on Lower-Frequency Sidemode Injection-Locked Technique with an injection power level of 4.8 dBm.

Wen et al [8] proved that Injection-locking enhances the resonance frequency of the laser and the electrical feedback achieves strong resonance at the base-rate frequency of the injected data streams.

Our paper is based on directly modulated transport system which employs the external light-injection technique. The external light-injection technique greatly enhances the frequency response of the laser diode, and thus improves the overall performance of the fibre optical CATV system. The idea is implemented using Optisystem 10.0 and we analyse how the output power varies with and without the external light-injection technique. Using external light-injection technique we are analysing how the output power varies with 3dBm, 4dBm, 5 dBm and 8 dBm external injected power.

## **III.INTRODUCTION TO THE EXTERNAL-LIGHT INJECTION TECHNIQUE**

The recent changes in telecommunication regulations and changing market forces are making the market for broadband network services to the home an extremely lucrative and competitive area. Out of many competing technologies for such broadband services, major CATV companies are banking heavily on various methods of making the network more



# International Journal of Advanced Research in Electrical, Electronics and Instrumentation Engineering

(An ISO 3297: 2007 Certified Organization)

Vol. 3, Issue 12, December 2014

and more fast and efficient. Most of the interest exists in broadband network services to deliver a variety of products to consumers, such as Internet access, telephony, interactive TV, and video on demand. But due to its cost efficiency, we need to find a better way to do that. When we send any optical signal, we find there is some loss in the transmission and hence there is the loss in data. So to increase the fibre transmission distance, achieve high quality for the given system and increase the performance is the ultimate goal of the fibre optical cable television (CATV) transport systems. However, nonlinear distortions introduced by laser chirp, fibre dispersion effects can degrade the system performance as well as limit the maximum transmission distance. Till now many techniques have been devised to circumvent these problems, but many of them just increase the complexity of the system. In a recent study, external light-injection technique has been employed in a hybrid radio–fibre system to improve the bit-error-rate performance but it has not been employed as a system-performance improvement technique in an analog light wave system. We suggest that the external light injection technique can be used to meet all the goals of CATV system efficiently. The external light-injection technique can greatly enhance the frequency response of the laser diode. It is expected to have good performances in analog fibre optical CATV systems.

## IV. THE CATV NETWORK

A CATV network is made up of three main parts: the trunk, the feeder, and the customer drop. The trunk is usually intended to cover large distances of tens of miles. The feeder portion of the cable is used by the consumers for tapping signal. Its maximum length is only a few miles since energy is tapped off to feed homes (subscribers) which require relatively high power levels. The drop is the flexible cable which goes to the home and it has a maximum length of approximately 600 feet and is made up of lower quality co-axial cable than the feeder or trunk. Older generation CATV systems used co-axial cables in the trunk and feeder portions of the network and therefore experienced many problems related to (a) interference from spurious radiation, (b) distortions introduced by amplifiers and (c) limited bandwidth. Long-distance transmission of fibre AM-VSB 80-channel CATV systems is used widely and is spread throughout the cable industry. Whereas, the maximum transmission distance of such systems is still limited by RF parameters and it is difficult to obtain better CNR performance due to full channel loading. In an optical CATV system, the signal is directly or externally modulated with light wave before it communicates. Directly modulating signal with LD is an economic method whereas the transmission distance and performance are significantly limited by laser chirping issues. In order to provide an economic structure with advanced transmission performance in external modulation system, direct modulation method is often combined with other techniques or components to compose higher performance and lower cost CATV system. By increasing the wavelength numbers, major parts of CSO distortions from each communication band are automatically removed from each communication channel. External light technique in particular have been experimented and proved as efficient method to enhance laser output power and laser resonance frequency.

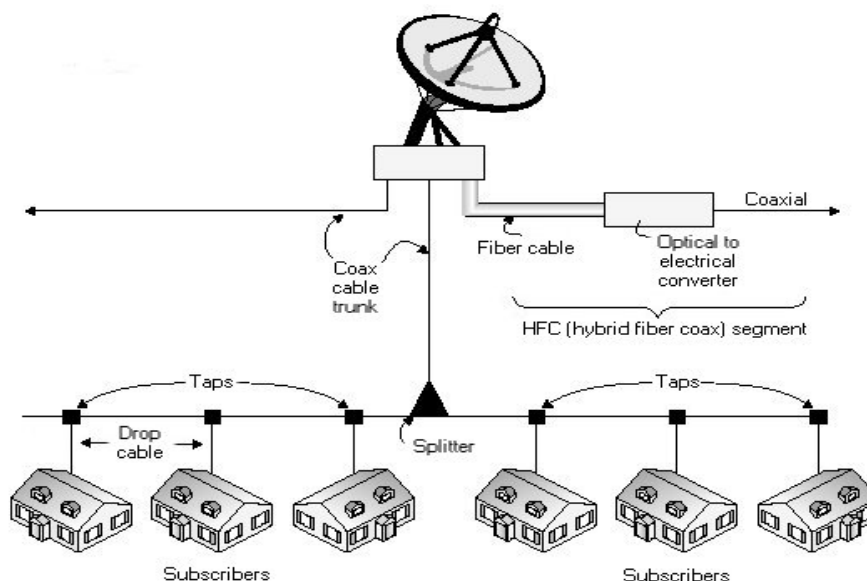


Fig. 1 General Block Diagram of CATV System

# International Journal of Advanced Research in Electrical, Electronics and Instrumentation Engineering

(An ISO 3297: 2007 Certified Organization)

Vol. 3, Issue 12, December 2014

## V. SIMULATION DESIGN

Our proposed directly modulated transport system employs the external light-injection technique. Without external light injection (Fig 3), CH 2-40 (ranging from 55 – 320 MHz) are directly fed into the first Continuous Wave (CW) laser diode and CH 41-78 (325 – 550 MHz) are directly fed into the second one. The CATV frequency bands are up-converted to the first microwave frequency bands (14.75 – 15.25 GHz) and then fed into the Continuous Wave (CW) laser diodes. The second CATV frequency bands are up-converted to the second microwave frequency bands (18.25 – 18.75 GHz) and then fed into the CW laser diodes. The central wavelengths of the two CW laser diodes are 1550.5nm and 1555.7nm, respectively. Without external light injection, the relative intensity noise (RIN) of the two CW laser diodes is about -170 dB/Hz. With external light injection, the RIN of the two DFB laser diodes are lower than -170 dB/Hz. Light is injected in the counter propagation direction through an optical isolator and a 3-dB optical coupler. The wavelengths of the injected light are 1550.7nm and 1555.6nm, respectively. In the system the optical power was coupled into the EDFA - I by a 2x1 optical coupler. After a 50 km single-mode fibre (SMF) transmission, the received optical signal was split by a 1x2 optical splitter, went through two separate optical band pass filters in order to select the appropriate wavelength, and detected using two broad-band analog optical receivers. This system can be used to increase the power of the sent signal to a larger extent while maintaining the efficiency at the same time.

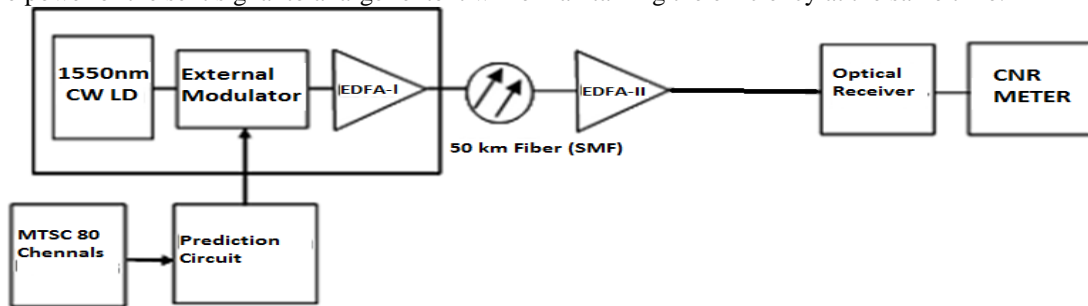


Fig. 2 Normal CATV system without external light-injection technique

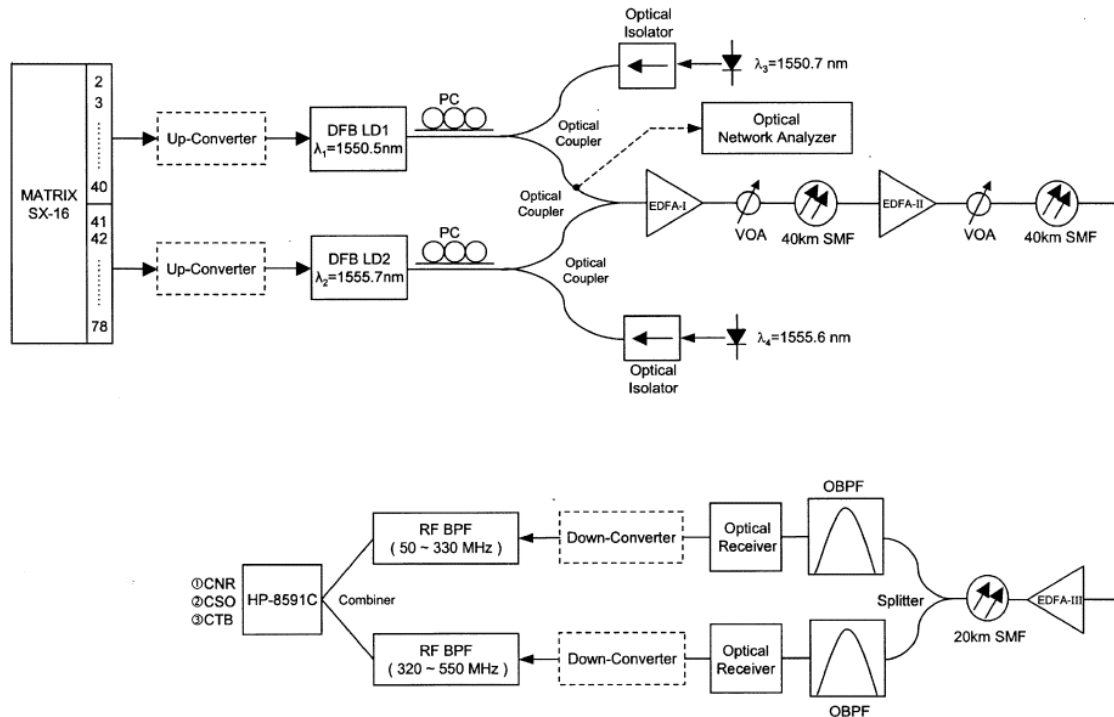


Fig. 3 Directly modulated CATV system employing external light-injection technique

## VI. SIMULATION, RESULT AND DISCUSSION

When the power injected into the laser diode is increased, the power launched into the EDFA-I is also increased. This is due to the fact that the external light injection will reduce the laser diode threshold current and hence increase the optical output power of the laser diode. The higher the input power launched into the EDFA, the better the CNR performance we can obtain in the system.

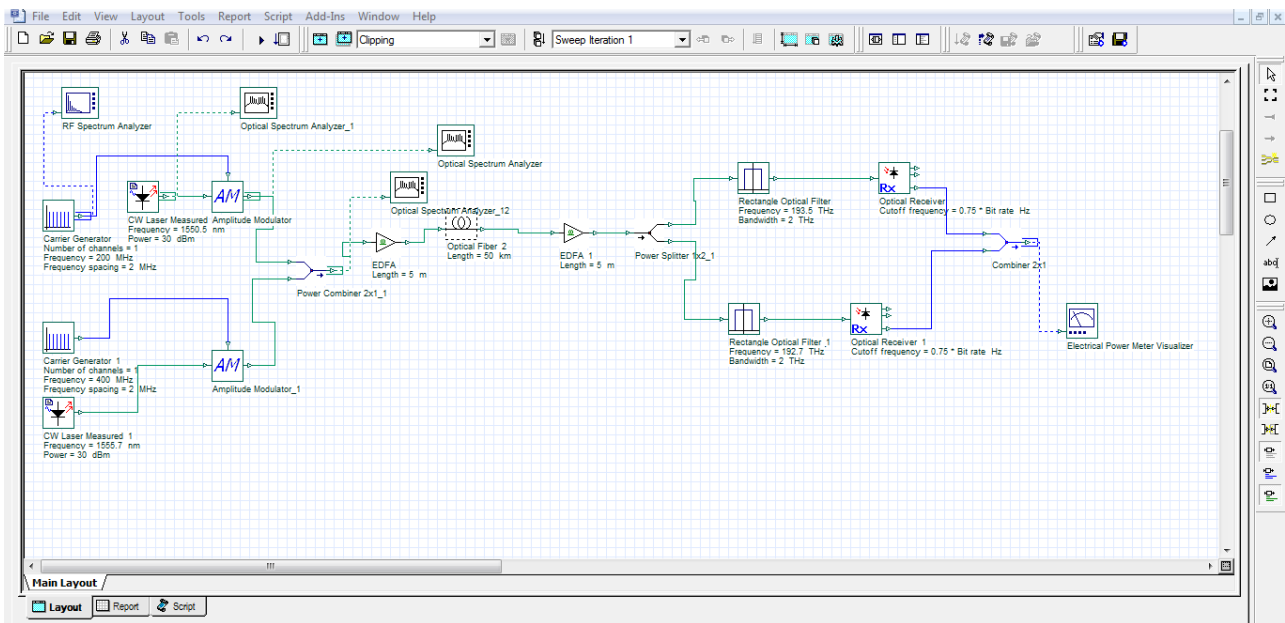


Fig. 4 CATV system without external light-injection technique simulated using Optisystem 10.0

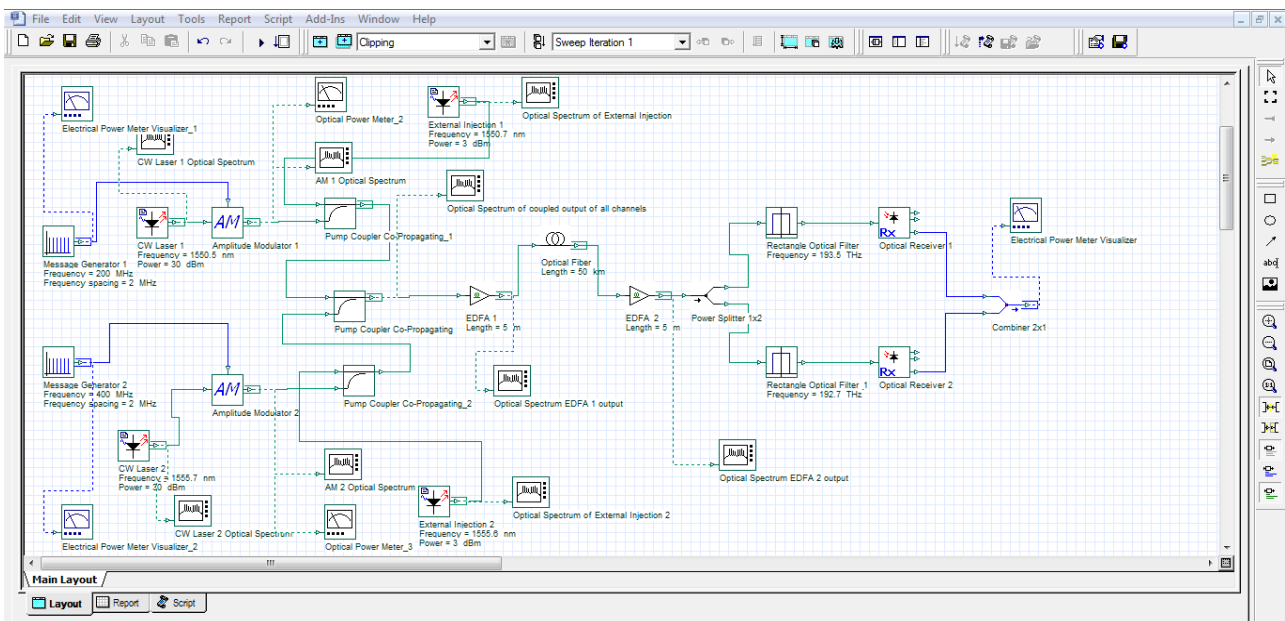


Fig. 5 CATV system employing external light-injection technique simulated using Optisystem 10.0

## International Journal of Advanced Research in Electrical, Electronics and Instrumentation Engineering

(An ISO 3297: 2007 Certified Organization)

**Vol. 3, Issue 12, December 2014**

INPUT POWER (dBm)	INJECTED POWER (dBm)	OUTPUT POWER (dBm)
30	None	2.34
30	3	4.45
30	4	5.21
30	5	6.53
30	8	8.34

Table. 1 Output to Injected Power Variation

In the normal case (without light injection) by using the 30dBm source light the electrical power output of the system is 2.34dBm . By using the 3dBm, 4dBm, 5 dBm and 8 dBm external light injection technique the electrical power output is 4.45dBm, 5.21dBm, 6.53 dBm and 8.34 dBm respectively.

A plot of ‘Injected Power’ vs ‘Output Power’ is shown below. This plot concludes that as injected power through the external light injection technique is increased then the output power also increases.

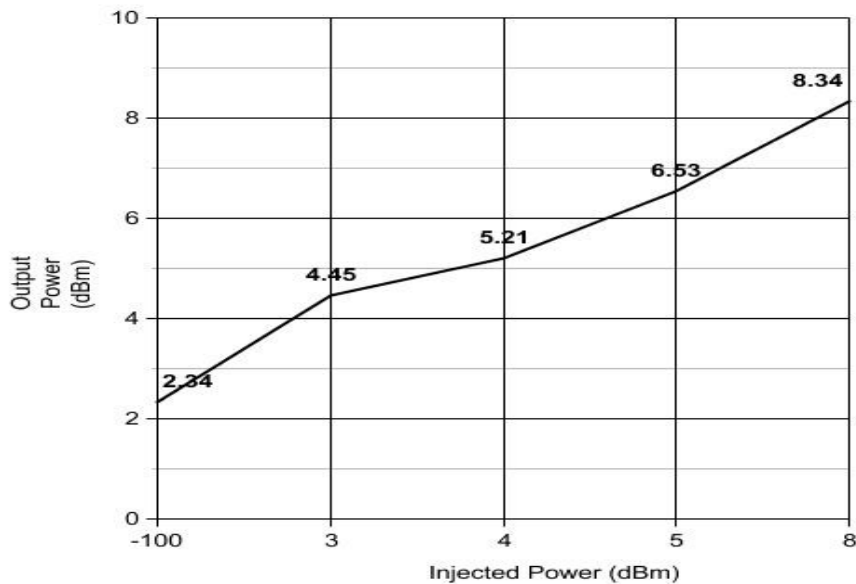


Fig. 5 Graphical Variation of Output to Injected Power

The output power as seen through a ‘Electrical Power Meter Visualizer’ for a CATV system without external light injection is shown below.



Fig. 6 Electrical Power Output (Without Injection)

# International Journal of Advanced Research in Electrical, Electronics and Instrumentation Engineering

(An ISO 3297: 2007 Certified Organization)

Vol. 3, Issue 12, December 2014

The output power as seen through a ‘Electrical Power Meter Visualizer’ for a CATV system employing external light injection (3dBm injection) is shown below.



Fig. 7 Electrical Power Output (With 3dBm Injection)

The output power as seen through a ‘Electrical Power Meter Visualizer’ for a CATV system employing external light injection (4dBm injection) is shown below.



Fig. 8 Electrical Power Output (With 4dBm Injection)

The output power as seen through a ‘Electrical Power Meter Visualizer’ for a CATV system employing external light injection (5dBm injection) is shown below.



Fig. 9 Electrical Power Output (With 5dBm Injection)

The output power as seen through a ‘Electrical Power Meter Visualizer’ for a CATV system employing external light injection (8dBm injection) is shown below.



Fig. 10 Electrical Power Output (With 8dBm Injection)





# International Journal of Advanced Research in Electrical, Electronics and Instrumentation Engineering

(An ISO 3297: 2007 Certified Organization)

Vol. 3, Issue 12, December 2014

## VII.CONCLUSION

We propose and demonstrate a directly modulated AM- CATV EDFA-repeated system that uses the external light-injection technique to improve the systems' performance. The external light-injection technique greatly enhances the frequency response of the laser diode, and thus improves the overall performance of the fibre optical CATV system. The efficiency of the CATV system can be further increased by feeding the customers using the optical fibre i.e. fibre to home in place of coaxial cable. This can increase the efficiency by 10 times as compared to normal co-axial cable.

## REFERENCES

- [1] D. Piehler, C. Y. Kuo, J. Kleefeld, and C. Gall, "Nonlinear intermodulation distortion in an optically amplified analog video transport system with dispersion compensation fiber," in Eur. Conf. Opt. Communications, Paper WeP.02, pp. 3217–3220, 1996.
- [2] J. Helms, "Intermodulation and harmonic distortions of laser diodes with optical feedback," J. Lightwave Technol., vol. 9, pp. 1567–1575, Nov.1991.
- [3] S. H. Lee, J. M. Kang, I. H. Choi, and S. K. Han, "Linearization of DFB laser diode by external light-injected cross-gain modulation for radio-over-fiber link," IEEE Photon. Technol. Lett., vol. 18, no. 14, pp. 1545–1547, Jul. 15, 2006.
- [4] Y. Hong and K. A. Shore, "Locking characteristics of a side-mode injected semiconductor laser," IEEE J. Quantum Electron., vol. 35, no. 11, pp. 1713–1717, Nov. 1999.
- [5] S. K. Mondal, B. Roycroft, P. Lambkin, F. Peters, B. Corbett, P. Townsend, and A. Ellis, "A multiwavelength low-power wavelength- locked slotted Fabry-Pérot laser source for WDM applications," IEEE Photon. Technol. Lett., vol. 19, no. 10, pp. 744–746, May 15, 2007.
- [6] X. J. Meng, T. Chau, and M. C. Wu, "Experimental demonstration of modulation bandwidth enhancement in distributed feedback lasers with external light injection," Electron. Lett., vol. 34, pp. 2031–2032, 1998.
- [7] Lu, H.-H., Patra, A. S., Tzeng, S.-J., Peng, H.-C., and Lin, W.-I., "Improvement of Fiber-Optical CATV Transport Systems Performance Based on Lower-Frequency Sidemode Injection-Locked Technique," IEEE Photonics Technology Letters 20, 351-353, 2008.
- [8] Attygalle, M., and Wen, Y. J. , "Injection-locked Fabry-Perot laser with electronic feedback for clock recovery from high-speed OTDM signals," IEEE Photonics Technology Letters 18, pp. 478-480, 2006.
- [9] Choi, K. M., Baik, J. S., and Lee, C. H. , "Broad-band light source using mutually injected Fabry-Perot laser diodes for WDM-PON," IEEE Photonics Technology Letters 17, pp. 2529-2531, 2005.
- [10] Hann, S., Kim, D. H., and S., P. C. , "Uni-lambda bidirectional 10/1.25 GbE access service based on WDM-PON," Electronics Letters 40, pp.194-195, 2004.
- [11] Ni, Y., Zhang, L., An, L., Peng, J., and Fan, C., "Dual-core photonic crystal fiber for dispersion compensation," IEEE Photonics Technology Letters 16, pp. 1516-1518, 2004.
- [12] Lu, H.-H., Huang, H.-H., Su, H.-S., and Wang, M.-C., "Fiber Optical CATV System-Performance Improvement by Using External Light-Injection Technique," IEEE Photonics Technology Letters 15, pp. 1017-1019, 2003.
- [13] Kaszubowska, P. Anandarajah, and L. P. Barry, "Improved performance of a hybrid radio/fiber system using a directly modulated laser transmitter with external injection," IEEE Photon. Technol. Lett., vol.14, pp. 233–235, Feb. 2002.
- [14] H. H. Lu, C. T. Lee, and C. J. Wang, "Dispersion compensation in externally modulated transport system using chirped fiber grating as well as large effective area fiber," Opt. Eng., vol. 40, pp. 656–657, 2001.
- [15] Srinath, S. "Performance Analysis of 2.5 Gbps GPON," International Journal of Advanced Research in Electrical, Electronics and Instrumentation Engineering , Vol.3 , Issue.6, pp:10148-10155, June,2014,.
- [16] L. P. Shen, W. P. Huang, G. X. Chen, and S. S. Jian, "Design and optimization of photonic crystal fibers for broad-band dispersion compensation," IEEE Photon. Technol. Lett., vol. 15, pp. 540-542, 2003.
- [17] Y. J. Wen, C.-J. Chae, and H. F. Liu, "Time-domain polarization interleaving of signal to allow polarization-insensitive all-optical clock recovery," IEEE Photon. Technol. Lett., vol. 17, no. 6, pp. 1304–1306, Jun. 2005.
- [18] H. H. Lu, C. L. Ying, W. I. Lin, Y. W. Chuang, Y. C. Chi, and S. J. Tzeng, "CATV/ROF transport systems based on light injection/optoelectronic feedback techniques and photonic crystal fiber," Opt. Commun., vol. 273, pp. 389–393, 2007.
- [19] J. L. Thomas, "Cable Television Proof-Of-Performances," in Hewlett- Packard Professional Book, ch. 8, pp. 158–193,1998.
- [20] S. Kawanishi, "High bit rate transmission over 1 Tbit/s," IEICE Trans. Commun., vol. E84-B, no. 5, pp. 1135–1141, 2001.

## BIOGRAPHY



**S.SRINATH** is currently studying final year ( 8<sup>th</sup> Semester), B.Tech, ECE, School of Electronics Engineering in VIT University, Vellore, India.



# International Journal of Advanced Research in Electrical, Electronics and Instrumentation Engineering

(An ISO 3297: 2007 Certified Organization)

Vol. 3, Issue 6, June 2014

## Performance Analysis of 2.5 Gbps GPON

S.Srinath

B.Tech , Department of ECE, Vellore Institute Of Technology, Vellore, Tamilnadu, India

**ABSTRACT:** The ITU-T G.984 is Gigabit-capable Passive Optical Networks (GPON) standard. In this paper, 2.5 Gb/s GPON link is presented. The quality or performance of a digital communication system is specified by its BER or Q value with respect to other parameters such as receiver sensitivity . The system performance is presented through various parameters such as Q factor, eye diagram. The proposed models have the nominal bit rate 2.5 Gbit/s with required bandwidth. It implemented using Opti-System 7.0.

**KEYWORDS:** GPON, Bit Error Rate(BER), Q Factor, Eye Diagram.

### I.INTRODUCTION

Fiber optics uses light signals to transmit data. As this data moves across a fiber, there needs to be a way to separate it so that it gets to the proper destination. A passive optical network does not include electrically powered switching equipment and instead uses optical splitters to separate and collect optical signals as they move through the network. A passive optical network shares fiber optic strands for portions of the network. Powered equipment is required only at the source and receiving ends of the signal. GPON (Gigabit Passive Optical Network) network consists of three important units ie Optical Line Terminal (OLT), Optical Network Unit (ONU) and Optical Splitters. The data is transmitted from the central office to a single optical fibre which runs from the central office to the optical splitters. This splitter then divides the power into N separate paths that goes to different subscribers. The number of splitting paths can vary from 2 to 64. Optical Line Terminal is a device that serves as the service provider endpoint of a passive optical network. It has two main functions: To perform conversion between the electrical signals used by the service provider's equipment and the fiber optic signals used by the passive optical network. To coordinate the multiplexing between the conversion devices on the other end of that network (called Optical Network Units). Optical Network Unit is used in combination with an Optical Line Terminal (OLT). It is a device that terminates any one of the endpoints of a fiber to the premises network. It transforms incoming optical signals into electronics at a customer's premises. Optical Splitters are used to divide the incoming light beam from a single fiber into two or more fiber channels. GPON offers many advantages: It supports triple play service. It is a term for the provisioning of two bandwidth intensive service- high speed internet access and television and a less bandwidth demanding service, telephone over a single broadband connection. It has a high bandwidth transmission and long reach service coverage (20 km). Since PON uses the same fiber for upstream as well as downstream transmission, it utilizes WDM (Wave Division Multiplexing) for bidirectional transmission. It adopts two multiplexing techniques. In the downstream direction the data packets are transmitted in a broadcast manner. 1,490 nm wavelength is used for downstream traffic while in the upstream direction the packets are transmitted in a TDMA manner. The wavelength used for upstream traffic is 1310 nm. 1550 nm is reserved for overlay services, typically RF video (analog).

In this paper different characteristics like jitter, minimum Bit Error Rate (BER), Q factor and optical power for different wavelengths are compared. We will also see the variation of these factors when there is a change in the fiber attenuation.

### II.RELATED WORK

While previous survey and research papers focussed on the downstream performance of a GPON system for data rates less than 2Gbps, this paper focuses on both the upstream and downstream performance of a GPON for data rate above 2Gbps ie 2.5Gbps(ITU-T G.984.1 standard). Higher data rate simulation is performed in this paper as high speed GPON network are the need of the hour. The performance measure of a GPON system presented in this paper analyses how the BER , Q-Factor and Optical power changes as wavelength and attenuation changes and how effective these factors are for better communication. The downstream performance analysis of GPON system is analysed for 'single user' case

# International Journal of Advanced Research in Electrical, Electronics and Instrumentation Engineering

(An ISO 3297: 2007 Certified Organization)

Vol. 3, Issue 6, June 2014

and ‘multiple user’ case. The upstream performance analysis of GPON system is analysed for ‘multiple user’ case. For analysing the performance of multiple user GPON system ‘Bi-Directional Optical Fibres’, ‘Bi-Directional Circulators’ and ‘Bi-Directional Splitters’ available in Optisystem 7.0 software were used.

### III. THEORY

Bit Error Rate (BER) is defined as the number of bit errors is the number of received bits of a data stream over a communication channel that has been altered due to noise, interference, and distortion or bit synchronization errors. BER is the number of bit errors divided by the total number of transferred bits during a studied time interval ie  $BER = \frac{E(t)}{N(t)}$  where E(t) is the number of bits received in error over time t, and N(t) is the total number of bits transmitted in time t. BER is a unit less performance measure, often expressed as a percentage. Q Factor describes how under damped an oscillator or resonator is. Higher Q factor indicates a lower loss of energy. Higher Q indicates a lower rate of energy loss relative to the stored energy of the resonator. A high-Q tuned circuit in a radio receiver would have more selectivity and hence better job of filtering out signals from other stations that lie nearby on the spectrum. Eye Diagram patterns are a widely used tool for studying the quality and stability of optical communication systems. The quality of the signals can be judged from the appearance of the eye. It is an experimental tool for the evaluation of the combined effects of channel noise and inter symbol interference on the performance of a baseband pulse-transmission system. It is the synchronized superposition of all possible realizations of the signal of interest viewed within a particular signaling interval. It is a composite view of all the bit periods of a captured waveform superimposed upon each other. If the bottom appears to have a smaller amplitude variation than the top, the signal seems to carry more 0s than 1s.

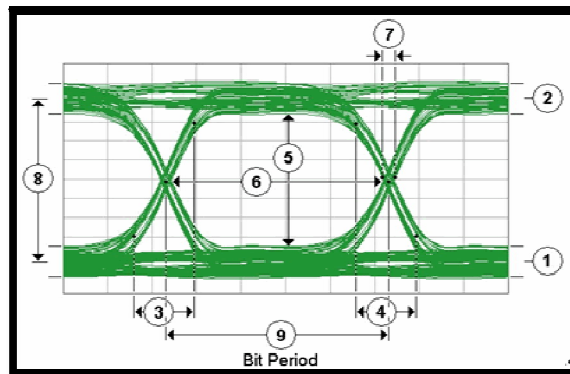


Fig.3.1. Eye Diagram

The following can be obtained from an eye diagram.

1	Zero level	Zero Level is a measure of the mean value of the logical 0 of an eye diagram.
2	One level	One Level is a measure of the mean value of the logical 1 of an eye diagram
3	Rise time	Rise time is a measure of the transition time of the data from the 10% level to the 90% level on the upward slope of an eye diagram.
4	Fall time	Fall time is a measure of the transition time of the data from the 90% level to the 10% level on the downward slope of an eye diagram
5	Eye height	Eye height is a measure of the vertical opening of an eye diagram. The eye height measurement determines eye closure due to noise.
6	Eye width	Eye width is a measure of the horizontal opening of an eye diagram. Jitter may appear on the waveform and influence the eye opening.
7	Deterministic jitter	Deterministic jitter is the deviation of a transition from its ideal time caused by reflections relative to other transitions
8	Eye amplitude	Eye amplitude is the difference between the logic 1 level and the logic 0 level histogram mean values of an eye diagram.
9	Bit rate	Bit rate (data rate) is the inverse of bit period (1 / bit period). The bit period is a measure of the horizontal opening of an eye diagram at the crossing points of the eye.

Table 3.1. Definations

# International Journal of Advanced Research in Electrical, Electronics and Instrumentation Engineering

(An ISO 3297: 2007 Certified Organization)

Vol. 3, Issue 6, June 2014

## IV.OVERVIEW OF GPON SYSTEM

Recommendation ITU-T G.984.1 describes a flexible optical fibre access network capable of supporting the bandwidth requirements of business and residential services and covers systems with nominal line rates of 2.4 Gbit/s in the downstream direction and 1.2 Gbit/s and 2.4 Gbit/s in the upstream direction. Both symmetrical and asymmetrical (upstream/downstream) gigabit-capable passive optical network (GPON) systems are described. GPON standard defines a lot of different line transmission rates for downstream and upstream direction.

TRANSMISSION DIRECTION	BIT RATES
UPSTREAM	155.52Mb/s
	622.08Mb/s
	1244.8Mb/s
	2488.32Mb/s
DOWNSTREAM	1244.16Mb/s
	2488.32Mb/s

Table.4.1. Bit rates

The simulation was performed for a bit rate of 2.5Gbps.

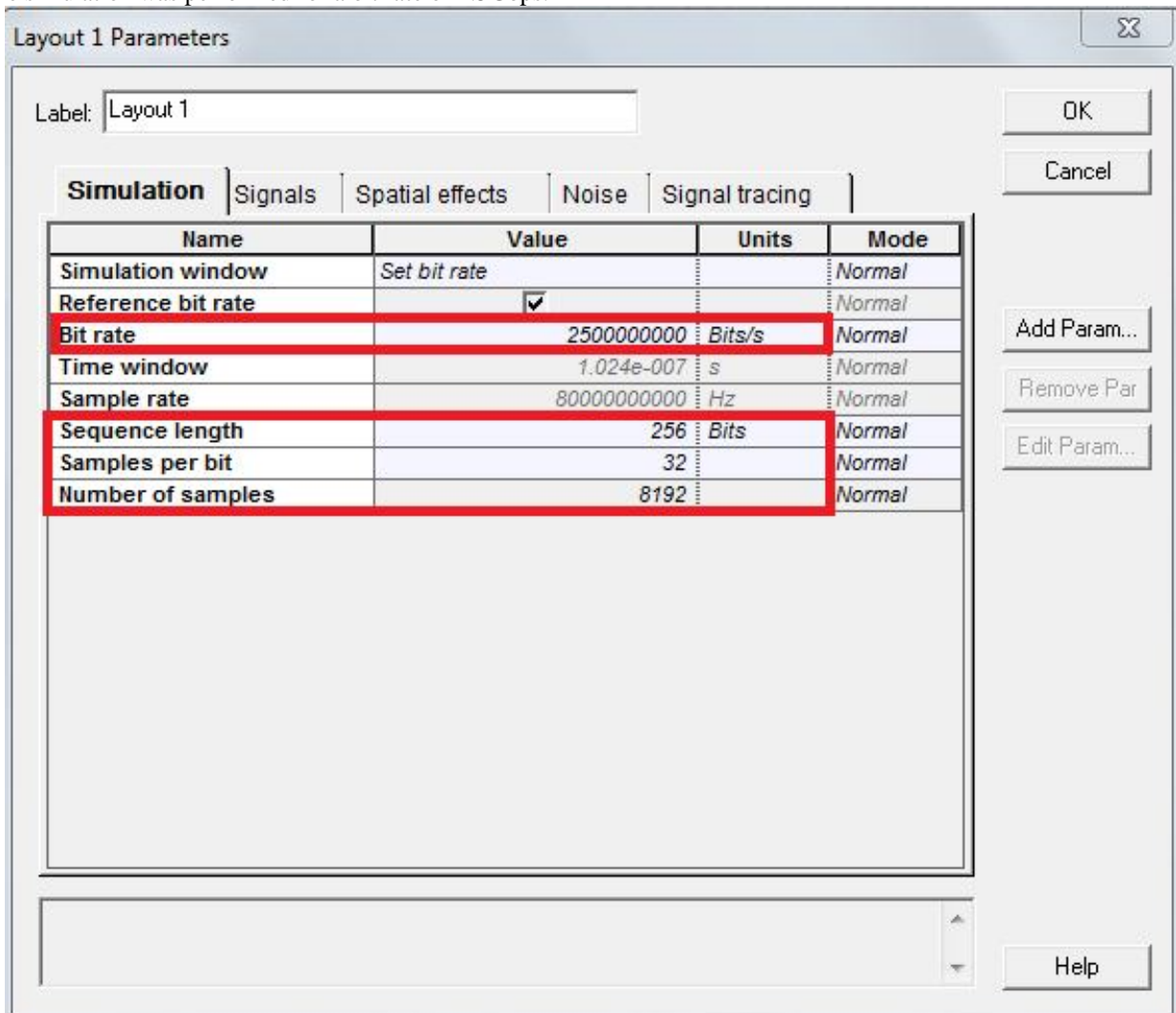


Fig.4.1. GPON simulation Properties

# International Journal of Advanced Research in Electrical, Electronics and Instrumentation Engineering

(An ISO 3297: 2007 Certified Organization)

Vol. 3, Issue 6, June 2014

## V.SIMULATION DESIGN, MODELING & RESULTS AND DISCUSSION

The proposed 2.5 Gbps simulation model of GPON was done in optisystem software. The model was designed for a ‘single user’ scenario and a ‘multiple user’ scenario. It consists of pseudo random sequence generator, NRZ pulse generator, continuous wave laser source, Mach-Zehnder modulator, It also has an ONT receiver should have photodiode, low pass filter, 3R generator, BER analyzer, Bessel optical fiber filter. The link, sometimes called channel, consists of 20 km/50km of single mode fiber SMF28 and optical attenuator so as to add the loss for all the ODN class.

### SINGLE USER :

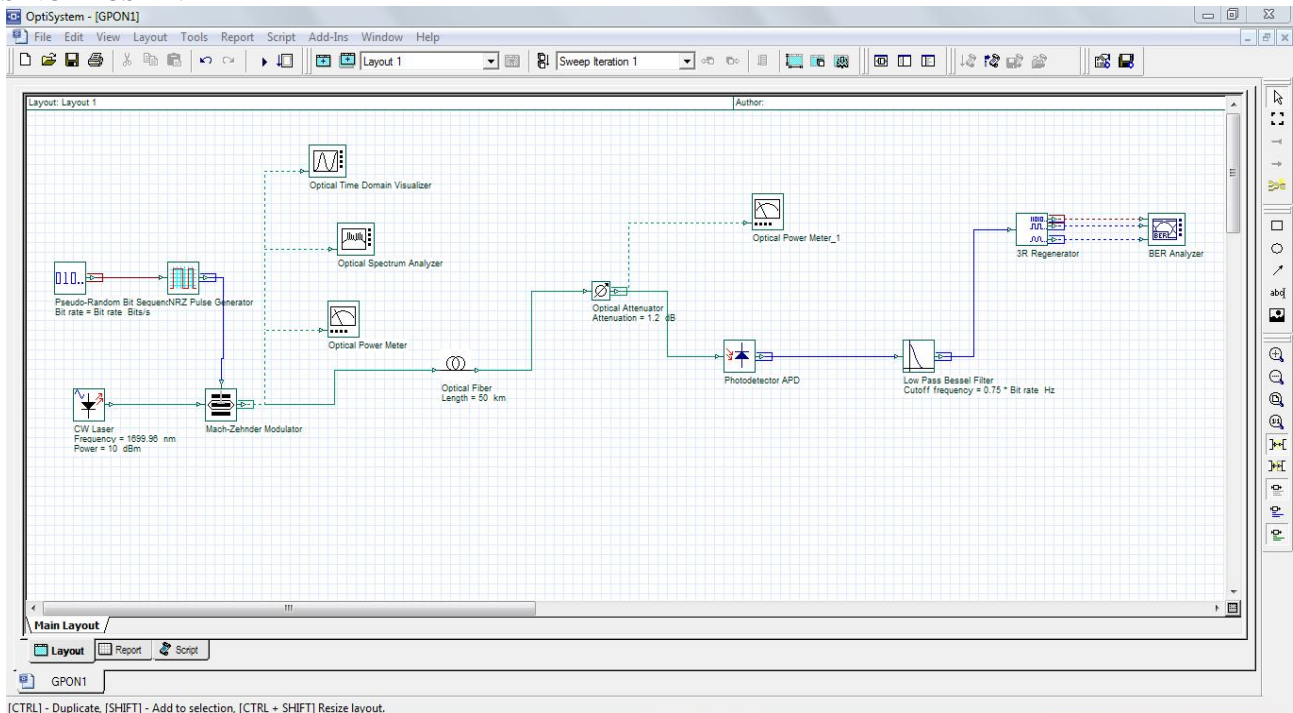


Fig.5.0. Downstream GPON simulation in Optisystem for Single User

### CASE 1:

In CASE 1 , the wavelength of 1490 nm was chosen with a fibre length of 50km and fibre attenuation of 0.7db/km.

JITTER	0.625 bit period	
Q FACTOR	5.22659	
MINIMUM BER	8.5987e-008	
OPTICAL POWER	Before transmission	6.785 dBm
	After transmission	-29.418 dBm

Table.5.1.Results Table

In figure 5.1 an open eye pattern is obtained which indicates less jitter and signal distortion. Figure 5.2 represents the Q factor which is high and its sharp graph indicates low loss. Figure 5.3 indicates the BER which is less. The optical power at the end of the fiber through which the signal has been transmitted has reduced from 6.75 dBm to -29.418 dBm.



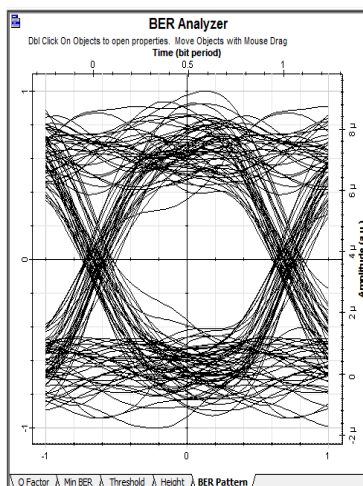


Fig.5.1.Eye Diagram

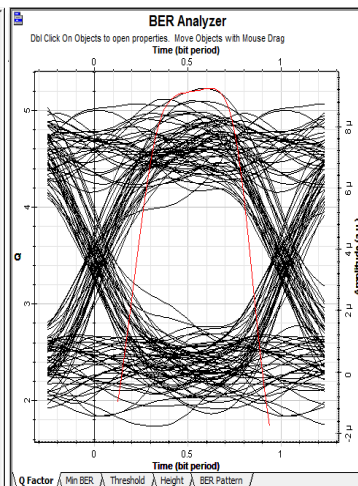


Fig.5.2.Q Factor

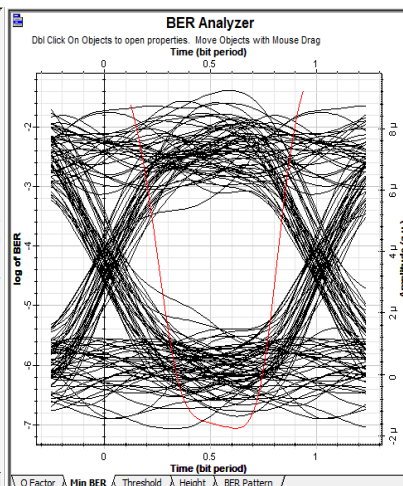


Fig.5.3.Min. BER

## CASE 2:

In CASE 2 , the wavelength of 1699.983 nm was chosen with a fibre length of 50km and fibre attenuation of 0.6db/km.

JITTER	0.0443748 bit period	
Q FACTOR	20.8075	
MINIMUM BER	3.02532e-07	
OPTICAL POWER	Before transmission	6.785 dBm
	After transmission	-24.501 dBm

Table.5.2. Results

Figure 5.4 has more number of amplitude variation at the one level than the zero level. Hence there are more number of one's in the signal than zero's. Figure 5.5 represents the Q factor which is around 20. Figure 5.6 indicates the BER which is low. The optical power at the end of the fiber through which the signal has been transmitted has reduced from 6.785 dBm to -24.501 dBm.

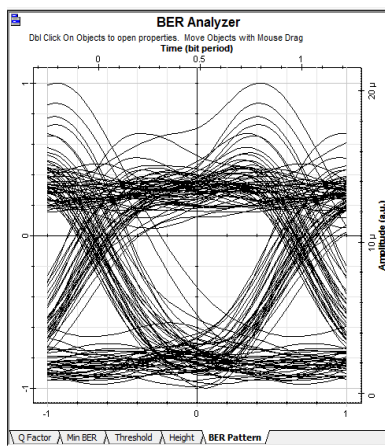


Fig.5.4.Eye Diagram

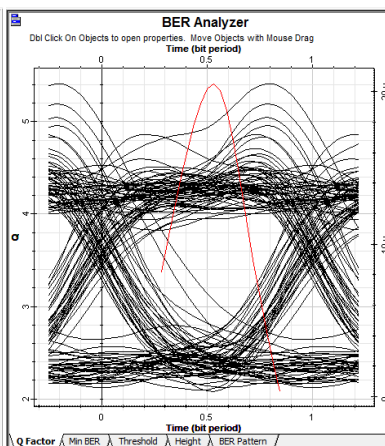


Fig.5.5.Q Factor

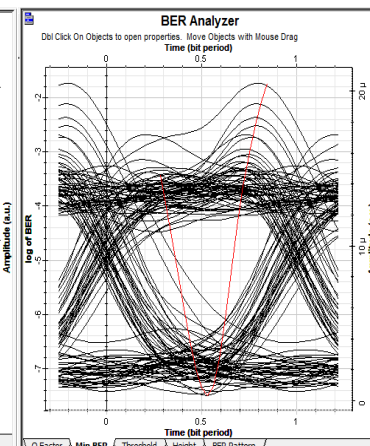


Fig.5.6.Min BER

# International Journal of Advanced Research in Electrical, Electronics and Instrumentation Engineering

(An ISO 3297: 2007 Certified Organization)

Vol. 3, Issue 6, June 2014

**CASE 3:**

In CASE 3 , the wavelength of 1700 nm was chosen with a fibre length of 50km and fibre attenuation of 0.2db/km.

JITTER	0.402938 bit period	
Q FACTOR	3.15213	
MINIMUM BER	0.000757	
OPTICAL POWER	Before transmission	6.785 dBm
	After transmission	-5.473 dBm

Table.5.3. Results

In figure 5.7 the eye opening is very small indicating lot of noise and crosstalk in the signal. Figure 5.8 represents the Q factor which is low. Figure 5.9 indicates the BER which too has increased from the previous cases. The optical power at the end of the fiber through which the signal has been transmitted has reduced from 6.785 dBm to -5.473 dBm.

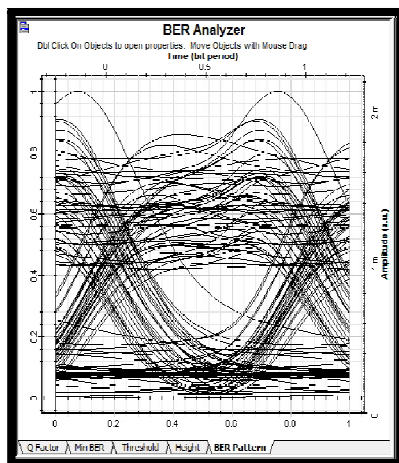


Fig.5.7.Eye Diagram

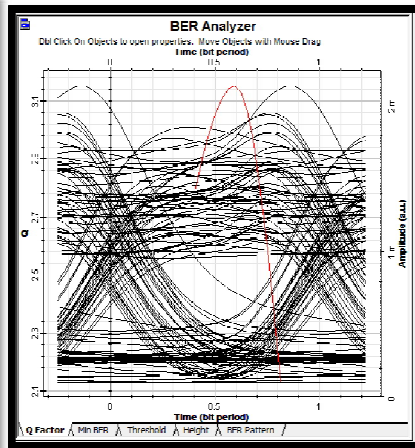


Fig.5.8.Q Factor

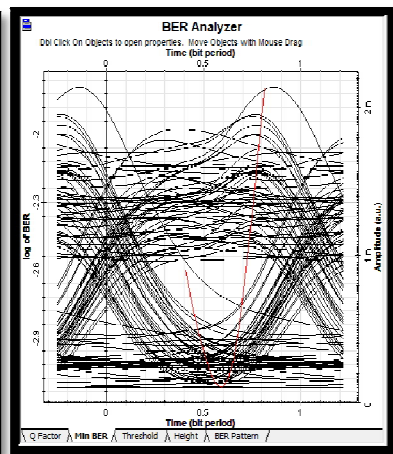


Fig.5.9.Min BER

**MULTIPLE USER:**

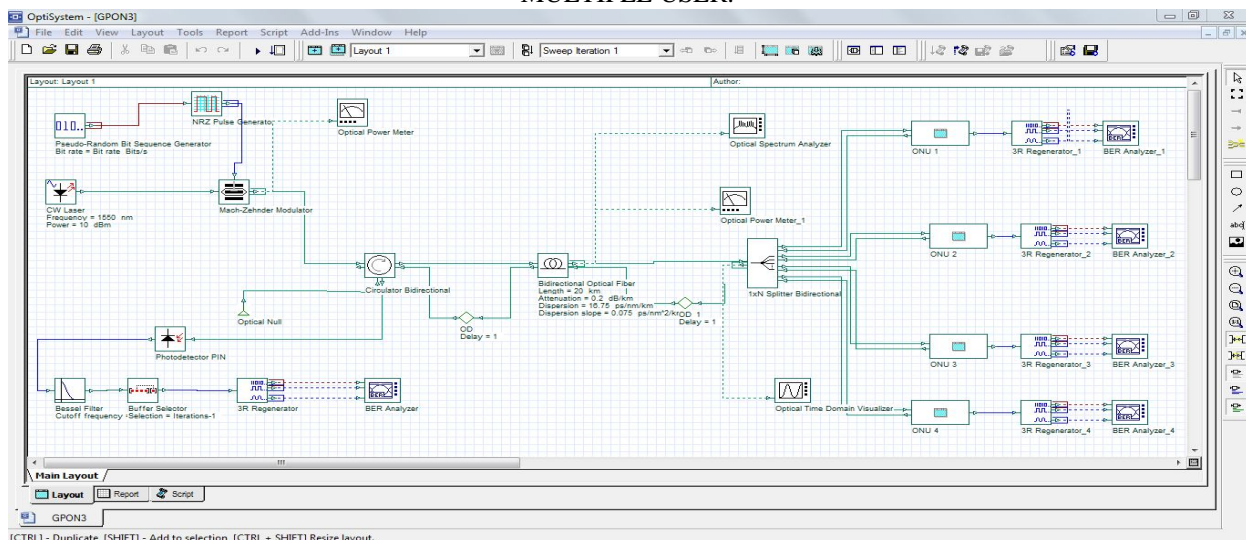


Fig.5.10. Bi-Directinal Link GPON simulation in Optisystem for Multiple User

# International Journal of Advanced Research in Electrical, Electronics and Instrumentation Engineering

(An ISO 3297: 2007 Certified Organization)

Vol. 3, Issue 6, June 2014

The wavelength of 1550 nm was chosen with a fibre length of 20km and fibre attenuation of 0.2db/km.

Power(dBm)	Wavelength(nm)	Maximum Q factor And BER At OLT	Maximum Q factor At ONU	Minimum Bit Error Rate At ONU
-3	1550	5.3621 – Q Fac.	7.11595 – ONU 1	5.53183e-013
		4.085e-008 -BER	7.37012 – ONU 2	8.47126e-014
			6.99794 – ONU 3	1.29797e-012
			6.99794 – ONU 4	1.29797e-012

Table.5.4 Results

In figure 5.11 an open eye pattern is obtained which indicates less jitter and signal distortion. Figure 5.12 represents the Q factor which is high and its sharp graph indicates low loss. Figure 5.13 indicates the BER is less. The optical power at the end of the fiber through which the signal has been transmitted has reduced from -6.172 dBm to -13.172 dBm.

Input Power :

Output Power :

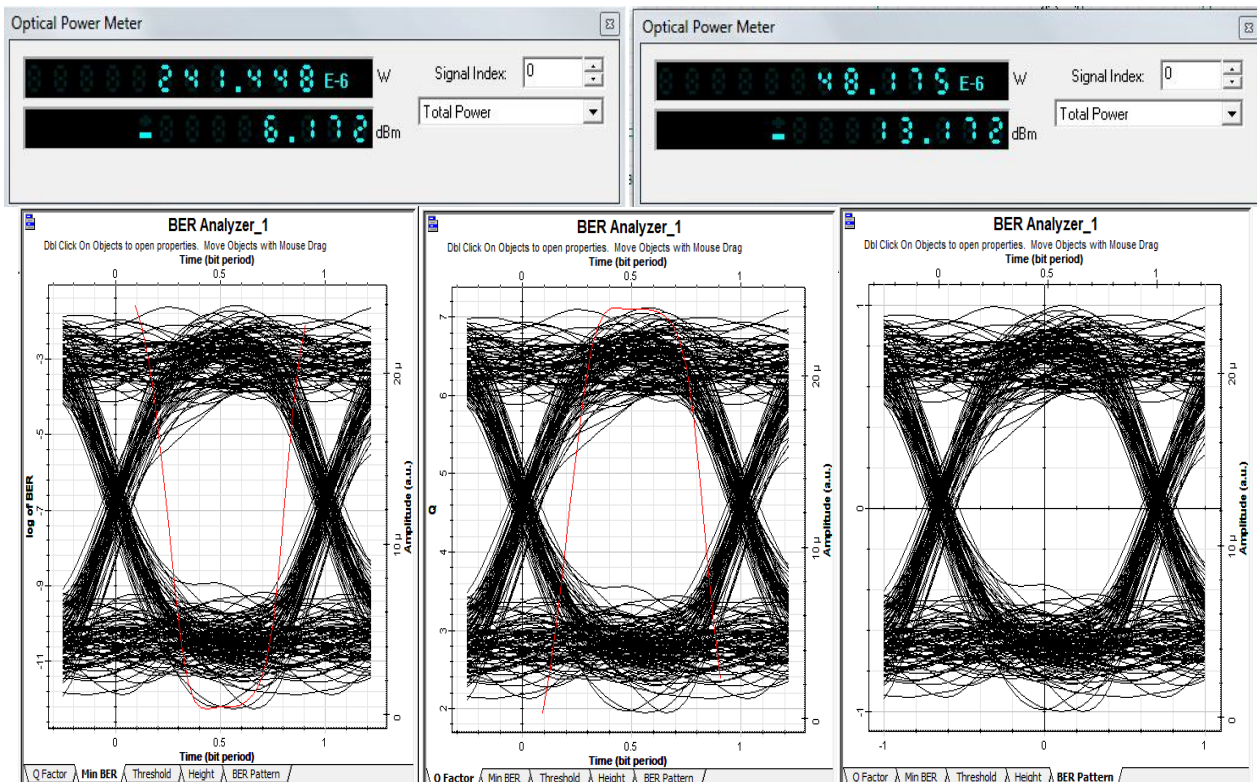


Fig.5.11.Min BER

Fig.5.12.Q factor

Fig.5.13. Eye Diagram

## VI.CONCLUSION

SINGLE USER - From the graphs we can see that as the wavelength is changed from 1490 nm to 1700 nm the eye diagram changes. In the first case i.e. 1490 nm an open eye pattern is obtained which indicates less jitter and signal distortion. The Q factor is high and its sharp graph indicates low loss. Also the BER is less. The optical power at the end of the fiber through which the signal has been transmitted has reduced from 6.75 dBm to -29.418 dBm.





# International Journal of Advanced Research in Electrical, Electronics and Instrumentation Engineering

(An ISO 3297: 2007 Certified Organization)

Vol. 3, Issue 6, June 2014

The second case 1699.983 nm has more number of amplitude variation at the one level than the zero level. Hence there are more number of one's in the signal than zero's. The jitter has increased from the previous cases. The Q factor has reduced to a mere 20 and there is a small BER too.

In the third case of 1700 nm, the eye opening is very small indicating lot of noise and crosstalk in the signal. There is a huge amount of jitter and it has a very low Q factor. The BER too has increased from the previous cases.

Thus performance of the network is best obtained at a wavelength of 1490 nm.

MULTIPLE USER USING BI-DIRECTIONAL LINK - From table 5.4, the wavelength was chosen to be 1550 nm in which Q factor was found out to be around 6 for the 'Optical network units' and the BER was found out to be  $10^{-12}$ . Similarly for the uplink Q factor was found out to be around 6 for the 'OLT' and the BER was found out to be  $10^{-8}$ . Thus, we see that the Q factor and the BER was exceptionally good for the GPON system operating at a wavelength of 1550nm and an input power of 10dbm using an optical fibre of length 20km with an attenuation of 0.2db/km.

## VIII. ACKNOWLEDGEMENT

At the outset, I would like to express my gratitude for my institute – Vellore Institute of Technology (V.I.T.) for providing me with the opportunity to undergo my undergraduate training, and assimilate knowledge and experience hitherto unknown to me. I would like to sincerely thank my teacher, **Prof. Revathi.S** - Assistant Professor (Selection Grade), for her constant support during the course of my activities. I will forever be obliged to madam for her assistance, encouragement and guidance.

## REFERENCES

- [1] X. Z. Qiu, J. Vandewege, F. Fredricx, and P. Vetter, "Burst Mode Transmission in PON Access Systems", 7th Eur. Conf. networks Optical Communication, pp.127–132, 2002.
- [2] Xing-Zhi Qiu, "Development of GPON Upstream Physical-Media-Dependent Prototypes," Journal of Lightwave Technology, Vol.22, Issue.11, pp.2498 – 2508, 2004.
- [3] P. Vetter, "Study and Demonstration of Extensions to the Standard FSAN BPON" ,Int. Symp. Services Local Access, pp.119–128, 2002.
- [4] ITU-T recommendation G.984.1, "Gigabit-capable Passive Optical Networks (GPON): General Characteristics", International Telecommunication Union, March 2003.
- [5] ITU-T Recommendation G.984.2, "Gigabit-capable Passive Optical Networks (G-PON): Physical Media Dependent (PMD) layer specification", International Telecommunication Union, March 2003.
- [6] ITU-T Recommendation G.975, "Forward error correction for Submarine systems", International Telecommunication Union, Oct. 2000.
- [7] ITU-T recommendation G.984.4, "Gigabit-capable Passive Optical Networks (GPON): ONT management and control interface specification", International Telecommunication Union, June 2004.
- [8] Bakarman H.A. ,Shaari . S, Ismail.M , "Simulation of 1.25 Gb/s downstream transmission performance of GPON-FTTx", International Conference on Photonics (ICP), pp. 1 – 5, 2010
- [9] V. Alwayn, "Optical Network Design and Implementation", Cisco Press, 2004.
- [10] J. H. Franze and V. K. Jain, "Optical Communications: Components and Systems", Narosa Publishing House, 2000.
- [11] T. Antony and A. Gumaste, "WDM Network Design", Cisco Press, ch. 4, 2003.
- [12] Lallukka, Sami & Raatikainen, "Pertti. Passive Optical Networks. Transport concepts", Espoo, 2006.
- [13] F. J. Effenberger and E. Shraga, "Status of GPON and B-PON standards", Flexlight-networks, 2004.

## BIOGRAPHY



**S.SRINATH** Currently studying B.Tech, ECE, school of electronics engineering in VIT University, Vellore, India.

## Design and Electromagnetic Modeling of E-Plane Sectoral Horn Antenna For Ultra Wide Band Applications On WR-137 & WR-62 Waveguides

S.Srinath

(Final Year Student, ECE, Vellore Institute of Technology, Vellore, India)

---

**ABSTRACT** : The Design and EM modeling of a E-Plane Sectoral Horn Antenna for Ultra Wide Band Application on WR-137 and WR-62 standard waveguides are presented in this paper. In E-plane sectoral antenna, the E-Plane is much narrower as the flaring and dimensions of the horn are much greater in that direction. The horn flare angle, horn size, wall thickness, etc of the E-plane sectoral horn antenna are examined. The return loss, input impedance, total gain and field pattern of the E-plane sectoral horn antenna are observed. The antenna is simulated using ANSOFT HFSS 14.0.

**KEYWORDS** : Ansoft HFSS Simulator, Beam width, Directivity, E-Plane Horn Antenna, Electromagnetic modeling, Radiation Pattern, Return Loss

---

### I. INTRODUCTION

An antenna is an electrical device which converts electric currents into radio waves, and vice versa. To transmit the signal a transmitter applies an oscillating radio frequency electric signal to the antenna's terminals, and the antenna radiates the energy in the form of electromagnetic waves. Horn antennas are used as antennas at UHF and microwave frequencies, above 300 MHz. They are used as feeders for larger antenna structures such as parabolic antennas. Over the hundred years, horn antennas have given the best directive and high power operation for Microwave Frequencies. Design Simplicity and large gain with best matching properties are added advantage of Horn antenna. Applications include Radar, Satellite tracking, Radio astronomy and Communication dish antennas. Other applications are Reflector feeds, Gain standards for antenna measurements, EMC/EMI tests, Communication systems, Direction finding (DF), mm-wave systems.



Fig 1 : A Practical Horn Antenna

A E-plane sectoral horn is one in which the opening is flared in the direction of the E-field.

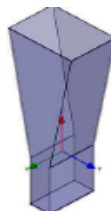


Fig 2 : E-Sectoral Horn Antenna

The E-Plane sectoral horn antennas are chosen because of their directional radiation pattern, ability to achieve high gain and directivity, and their ease of fabrication. The horn antenna which is designed was subject to the following constraints:



- Operating frequency around 8 GHz (C Band) for first case and 16 GHz (Ku Band) for second case.
- Maintain a gain of 10 dB over the entire operating frequency range

## II. ANTENNA DESIGN

The C and Ku frequency bands were selected as the operating frequency. These bands are selected as they pertain to the communication frequency bands. The design was performed to accomplish an ultra-wide bandwidth. (i) For the first case of 8GHz (C Band) the operating frequency was chosen to be 8GHz. The waveguide dimensions are  $a = 34.85\text{mm}$ ,  $b = 15.8\text{mm}$ , waveguide length = 31.75mm. These indicate the standard WR-137 waveguide. Horn size dimensions are  $b=44.45\text{mm}$ , horn flare length = 95.25mm, wall thickness = 1.626mm. (ii) For the second case of 16GHz (Ku Band) the operating frequency was chosen to be 16GHz. The waveguide dimensions are  $a = 15.8\text{mm}$ ,  $b = 7.9\text{mm}$ , waveguide length = 15.88mm. These indicate the standard WR-62 waveguide. Horn size dimensions are  $b=22.23\text{mm}$ , horn flare length = 47.63mm, wall thickness = 1.016mm. For both the cases the outer boundary condition is Radiation Boundary Condition. The Radiation Boundary Condition are as follows :

- Absorption achieved via 2nd order radiation boundary
- Place at least  $\lambda/4$  from strongly radiating structure
- Place at least  $\lambda/10$  from weakly radiating structure
- The radiation boundary will reflect varying amounts of energy depending on the incidence angle. The best performance is achieved at normal incidence. Avoid angles greater than  $\sim 30^\circ$ . In addition, the radiation boundary must remain convex relative to the wave

In HFSS to properly model the far field behavior of an antenna, an appropriate volume of air must be included in the simulation. Truncation of the solution space is performed by including a radiation boundary condition on the faces of this air volume that mimics free space. The appropriate distance between strongly radiating structures and the nearest face of the air volume depends upon whether a radiation boundary condition is used. HFSS also uses Finite Element Method (FEM) as analysis & solution to Electromagnetic problems by developing technologies such as tangential vector finite elements, adaptive meshing, and Adaptive Lanczos-Pade Sweep (ALPS).

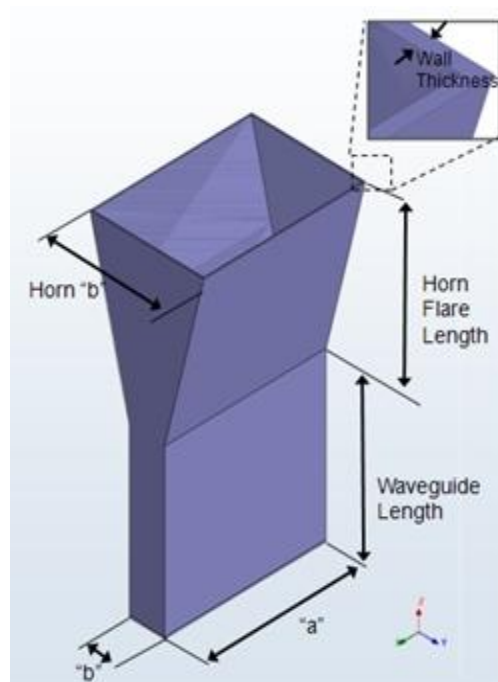


Fig 3 : Structure of the proposed E-Plane Horn Antenna

## III. PROPOSED MODEL IN ANSOFT HFSS 14.0 FOR CASE 1

The 3D view of the designed E-Plane Horn Antenna in HFSS for a solution frequency of 8GHz (C-Band) is shown below. The boundaries for the air-box are set as an ideal propagation space and the ground plane as perfect electric conductor.

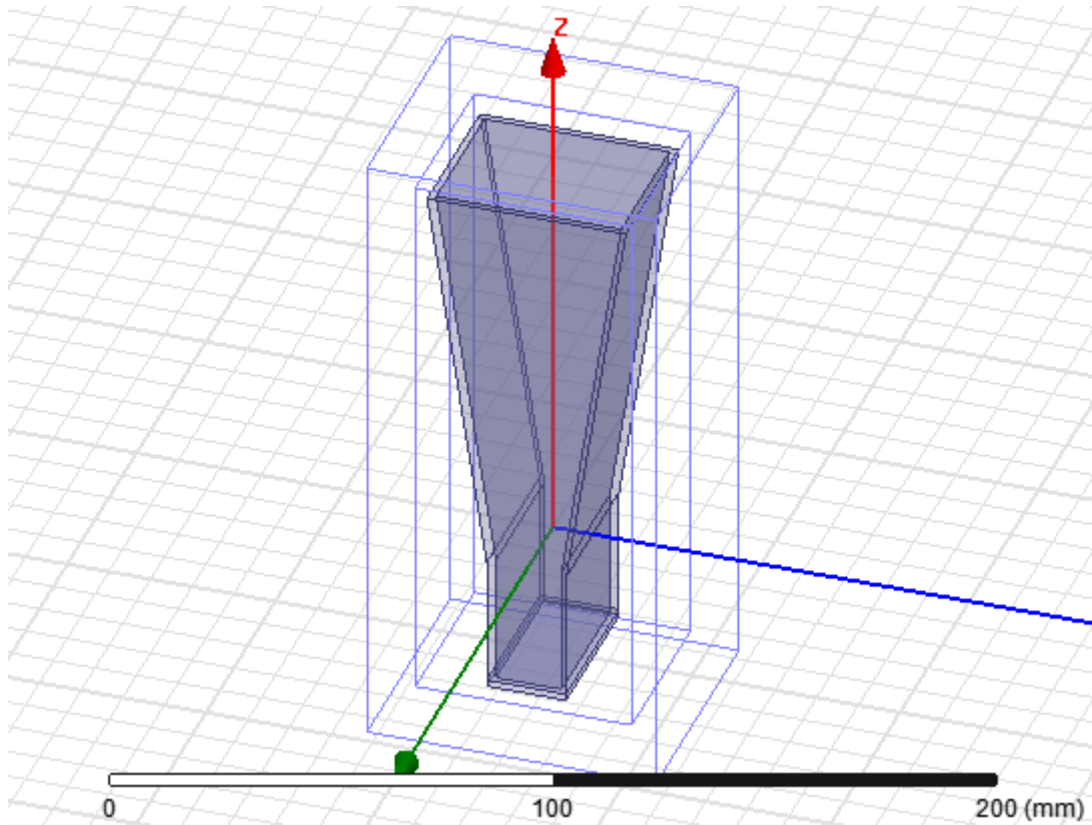


Fig 4 : 3D View of the E-Plane Horn antenna in HFSS for a solution frequency of 8Ghz

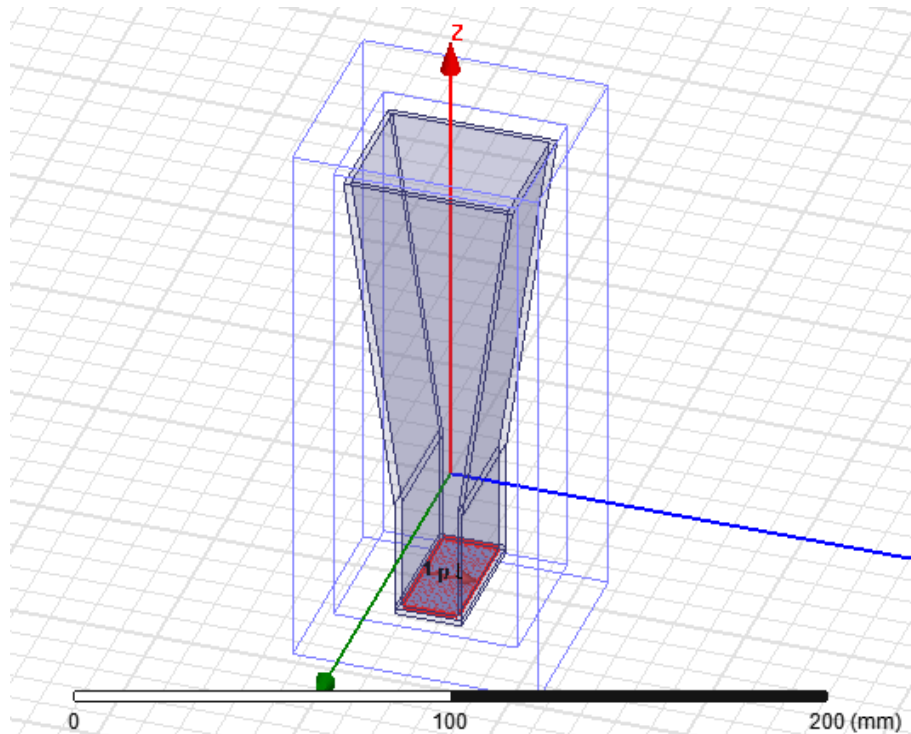


Fig 5 : Figure showing the direction of excitation for a solution frequency of 8Ghz

#### IV. RESULTS AND DISCUSSION FOR CASE 1

The parameters which verify the success of antenna design are beam width, impedance matching , etc. These are analysed here. The gain of the antenna versus frequency with return loss is -44dB at 8Ghz is shown below.

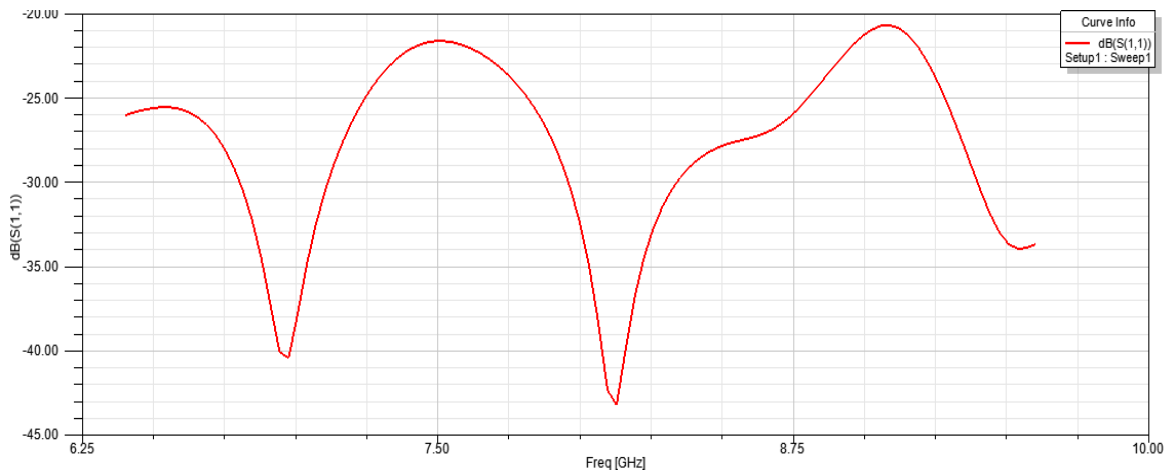


Fig 6 : Return loss in db over frequency range for a solution frequency of 8Ghz

The Radiation pattern for the antenna design in 3D is shown in below.

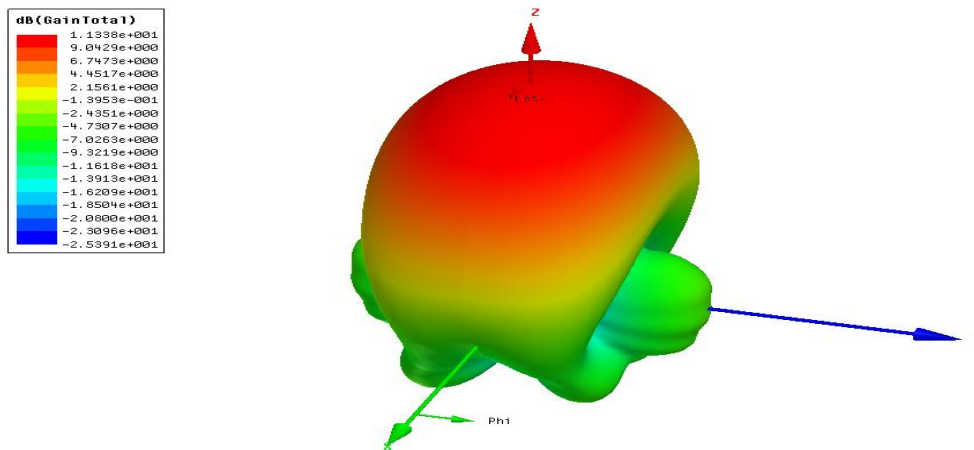


Fig 7 : 3D Radiation pattern of the antenna in HFSS for a solution frequency of 8Ghz

The 2D plot is total gain for phi = '0 deg' and phi = '90 deg' is shown below.

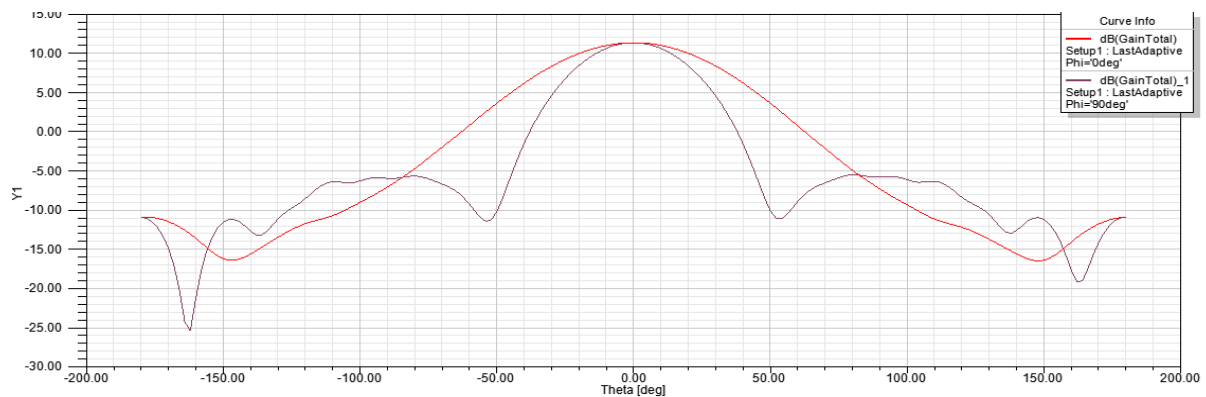


Fig 8 : 2D Plot for total gain versus theta (deg) with phi for a solution frequency of 8Ghz

**V. PROPOSED MODEL IN ANSOFT HFSS 14.0 FOR CASE 2**

The 3D view of the designed E-Plane Horn Antenna in HFSS for a solution frequency of 16Ghz (Ku-Band ) is shown below.

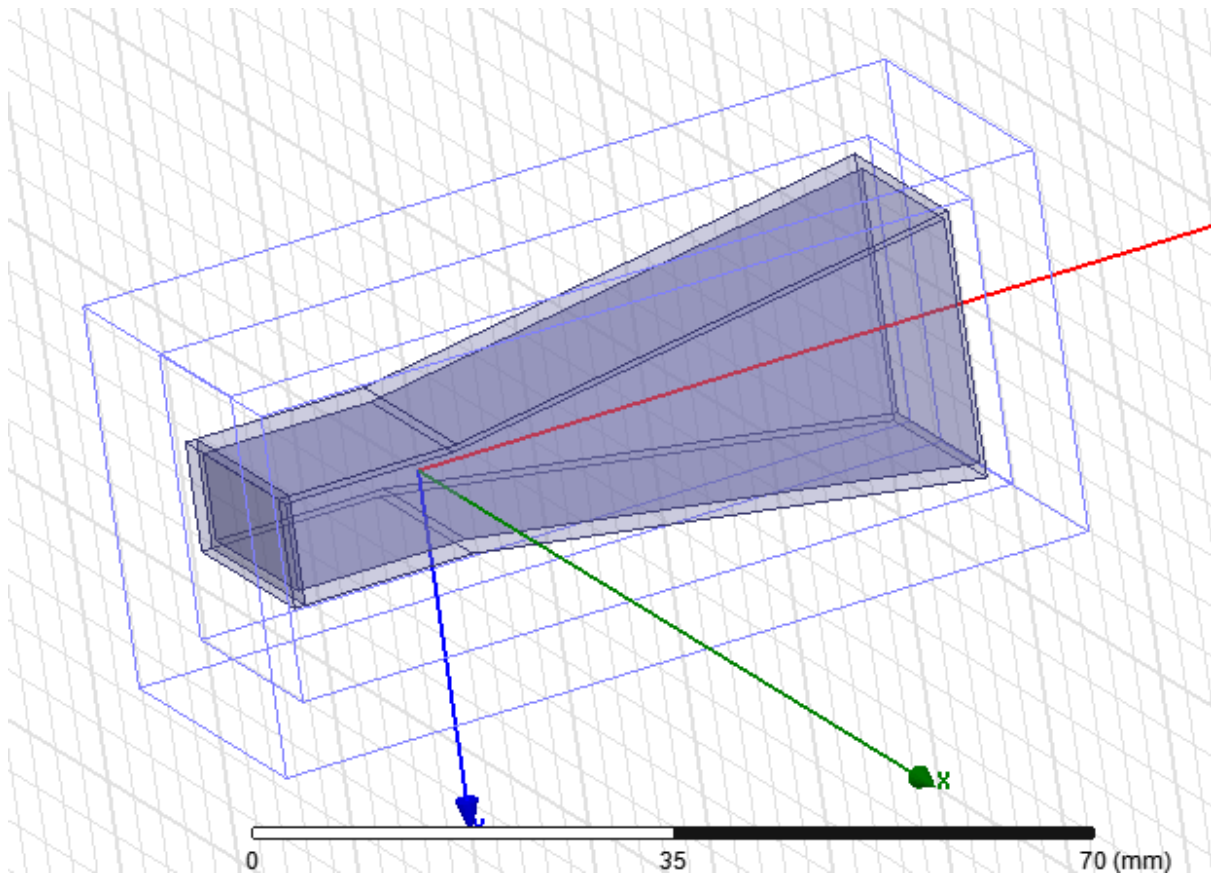


Fig 9 : 3D View of the E-Plane Horn antenna in HFSS for a solution frequency of 16Ghz

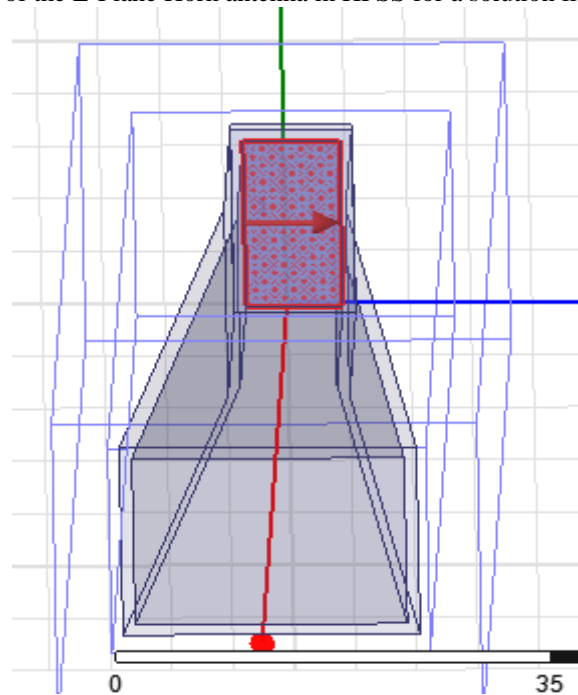


Fig 10 : Figure showing the direction of excitation for a solution frequency of 16Ghz

## VI. RESULTS AND DISCUSSION FOR CASE 2

The parameters which verify the success of antenna design are beam width, impedance matching , etc. These are analysed here. The gain of the antenna versus frequency with return loss is -49dB at around 16 Ghz is shown below.

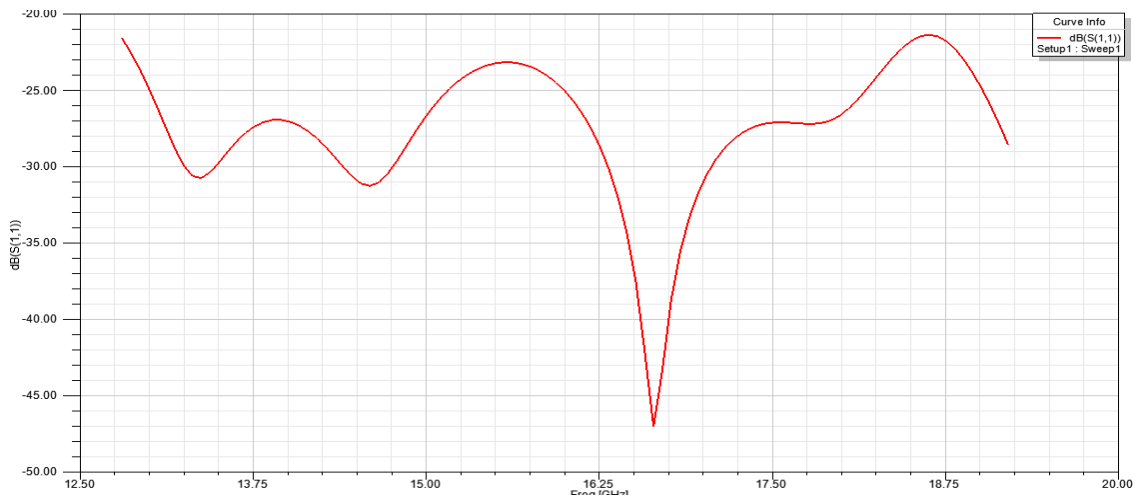


Fig 11 : Return loss in db over frequency range for a solution frequency of 16Ghz

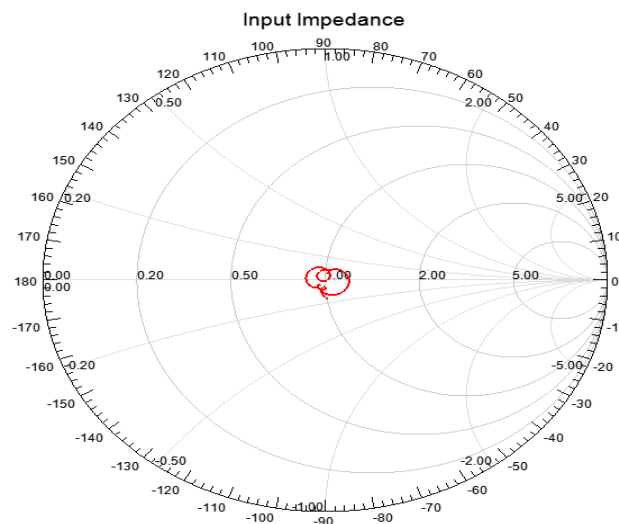


Fig 12 : The range of input impedance is shown below for a solution frequency of 16Ghz

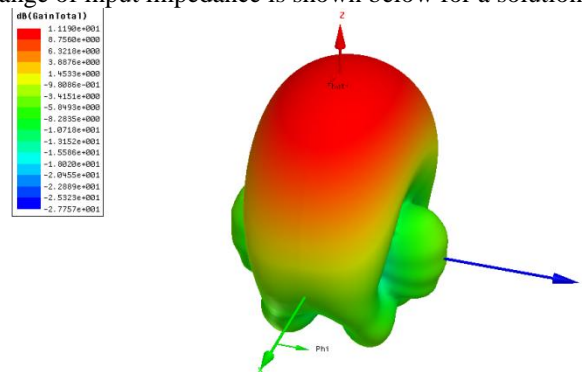


Fig 13 : 3D Radiation pattern of the antenna in HFSS for a solution frequency of 16Ghz



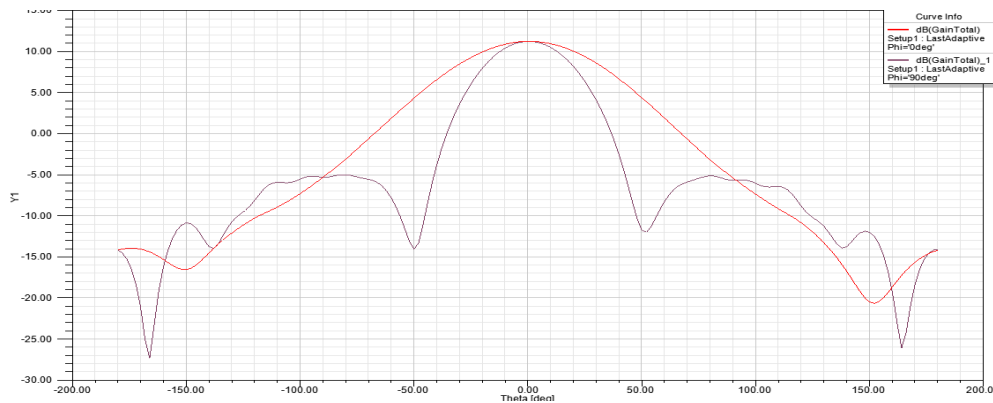


Fig 14 : 2D Plot for total gain versus theta (deg) with phi for a solution frequency of 16Ghz

## VII. CONCLUSION

An Ultra Wide Band E-Plane sectored Horn Antenna operating at solution frequencies of 8Ghz and 16Ghz frequency range was designed. The horn antenna which was designed satisfied the following constraints: (i)Operating frequency around 8 GHz (C Band) for first case and 16 GHz (Ku Band) for second case; (ii)Maintain a gain of 10 dB over the entire operating frequency range. The return loss for both the cases was found to be greater than -40db. Thus the desired results are achieved and the simulated structures are suitable for various applications.

## VIII. ACKNOWLEDGEMENTS

At the outset, I would like to express my gratitude for my institute – Vellore Institute of Technology (V.I.T.) for providing me with the opportunity to undergo my undergraduate training, and assimilate knowledge and experience hitherto unknown to me.

## REFERENCES

- [1] Lei Yang, Weihua Tan, Zhongxiang Shen, and Wen Wu, Wide-Band Wide-Coverage Linear Array of Four Semi-Circular Sector Horns, *IEEE transactions on antennas and propagation*, vol. 60, no.8, August 2012.
- [2] Thomas A Milligan, *Modem Antenna Design* (John Wiley & Sons INC, Second Edition.)
- [3] Constantine. A. Balanis, *Antenna Theory Analysis & Design* (John Wiley, & Sons INC, Third Edition.)
- [4] M. M. Tentzeris, J. Laskar, J. Papapolymerou, S. Pinel, V. Palazzari, R. Li, G. DeJean, N. Papageorgiou, D. Thompson, R. Bairavasubramanian, S. Sarkar, and J.-H. Lee, 3D Integrated RF and millimeter-wave functions and modules using liquid crystal polymer (LCP) system-on-package technology, *IEEE Trans. Adv. Packag.*, vol. 27, no. 2, pp. 332–340, May 2004.
- [5] D. M. Pozar and D. H. Schubert, *Microstrip Antennas—The Analysis and Design of Microstrip Antennas and Arrays* (New York: IEEE Press, 1995.)
- [6] F. Mohamadi Monavar, N. Komjani and P. Mousavi, Application of Invasive Weed Optimization to design a broadband Patch antenna with symmetric radiation Pattern, *IEEE antennas and wireless propagation letters*, Vol.10, 2011.
- [7] Qi wu, ronghong jin, and junping geng, A Single layer ultrawideband microstrip antenna, *IEEE antennas and wireless propagation letters*, vol.1, January 2010.
- [8] A. W. Love, *Antenna Engineering Hand book* (R. C. Johnson and H. Jasik, Ed. New York, 1984.)



## BIOGRAPHY

**S.SRINATH** passed 10<sup>th</sup> C.B.S.E. Board with a mark of 475/500(95%) and 12<sup>th</sup> C.B.S.E. Board from D.A.V. Boys Senior Secondary School, Gopalpuram, Chennai, India with a mark of 458/500(91.6%). Currently he is studying final year B.Tech, ECE, School of Electronics Engineering in Vellore Institute of Technology, Vellore, India.